EMODnet Thematic Lot n°2 Seabed Habitats

EASME/EMFF/2018/1.3.1.8/Lot2/SI2.810241

Start date of the project: 25/09/2019 - (24 months)

EMODnet Phase III

EUSeaMap 2019
A European broad-scale seabed habitat map
Technical Report

The European Marine Observation and Data Network (EMODnet) is financed by the European Union under Regulation (EU) No 508/2014 of the European Parliament and of the Council of 15 May 2014 on the European Maritime and Fisheries Fund.

Disclaimer

Document info

Title [ref]*	EUSeaMap 2019, A European broad-scale seabed habitat map, Technical Report
Authors [affiliation]	**Corresponding author** Mickaël Vasquez[f]; Mickael.Vasquez@ifremer.fr **Other authors** Eleonora Manca[i], Roberto Inghilesi[h], Simon Martin[f], Sabrina Agnesi[h], Zyad Al Hamdani[d], Aldo Annunziatellis[h], Trine Bekkby[k], Roland Pesch[a], Natalie Askew[i], Luis Bentes[b], Lewis Castle[i], Valentina Doncheva[g], Vivi Drakopoulou[e], Jorge Gonçalves[b], Leena Laamanen[l], Helen Lillis[i], Valia Loukaidi[e], Fergal McGrath[j], Giulia Mo[h], Pedro Monteiro[b], Mihaela Muresan[c], Eimear O'Keeffe[j], Jacques Populus[f], Jordan Pinder[i], Amy Ridgeway[i], Dimitris Sakellariou[e], Mika Simboura[e], Adrian Teaca[c], Fernando Tempera[f], Valentina Todorova[g], Leonardo Tunesi[h] and Elina Virtanen[l]. [a] Bioconsult Schuchardt&Scholle Gbr ("Bioconsult"), Reeder-Bischoff-Straße 54, 28757 Bremen, Germany [b] Centre of Marine Sciences ("CCMAR"), Universidade do Algarve, Campus de Gambelas, 8005-032 Faro, Portugal [c] National Institute of Research and Development for Marine Geology and Geoecology ("GeoEcoMar"), 23-25 Dimitrie Onciul Street, Sector 2, RO-024053, Bucharest, Romania

The European Marine Observation and Data Network (EMODnet) is financed by the European Union under Regulation (EU) No 508/2014 of the European Parliament and of the Council of 15 May 2014 on the European Maritime and Fisheries Fund.

	[d] Geological Survey of Denmark and Greenland ("GEUS"). Øster Voldgade 10, 1350, Copenhagen K, Denmark [e] Hellenic Centre for Marine Research ("HCMR"), Public Body, 46.7km Athens-Sounio Ave, Anavissos, 19013, Greece [f] Institut Français de Recherche pour l'Exploitation de la Mer ("Ifremer"), 1625 route de Sainte-Anne, Zone industrielle de la Pointe du Diable, 29280 Plouzané, France [g] Institute of Oceanology, Bulgarian Academy of Science ("IO-BAS"), First May Str 40, 9000 Varna, Bulgaria [h] Italian National Institute for Environmental Protection and Research ("ISPRA"), Via Vitaliano Brancati, 48 – 00144 – Roma – Italy [i] JNCC Support Co ("JNCC"), Monkstone House, City Road, Peterborough, Cambridgeshire, PE1 1JY, UK [j] Marine Institute, Rinville, Oranmore, Co. Galway, Ireland [k] Norwegian Institute for Water Research ("NIVA"), Gaustadallèen 21, NO-0349 Oslo, Norway [l] Finnish Environment Institute ("SYKE"), Mechelininkatu 34a, P.O. Box 140, 00251 Helsinki, Finland
Dissemination level	Public
Submission date	06/07/2020

Citation

This report should be cited as: **Vasquez M., Manca E., Inghilesi R., Martin, S., Agnesi S., Al Hamdani Z., Annunziatellis A., Bekkby T., Pesch R., Askew A., Bentes L., Castle L., Doncheva V., Drakopoulou V., Gonçalves J., Laamanen L., Lillis H., Loukaidi V., McGrath F., Mo G., Monteiro P., Muresan M., O'Keeffe E., Populus J., Pinder J., Ridgeway A., Sakellariou D., Simboura M., Teaca A., Tempera, F., Todorova V., Tunesi L. and Virtanen E. EUSeaMap 2019, A European broad-scale seabed habitat map, Technical Report, 2019.**

List of abbreviations and acronyms

CMEMS	Copernicus Marine Service
DTM	Digital Terrain Model
ESH	EMODnet Seabed Habitats
GIS	Geographic Information System
GLM	Generalised Linear Model
GTK	Geological Survey of Finland
HAT	Highest astronomical tide
IMR	Institute of Marine Research (Norway)
KdPAR	Attenuation coefficient of the PAR
LAT	Lowest astronomical tide
MSFD	Marine Strategy Framework Directive
NGU	Geological Survey of Norway
PAR	Photosynthetically Available Radiation
SDM	Species Dictribution Modeling

Executive summary

EUSeaMap 2019 is the third iteration of EUSeaMap. All versions have been produced as part of the EMODnet Seabed Habitats project, which is one of several thematic lots in EMODnet. The project has brought together a European consortium of specialists in benthic ecology and seabed habitat mapping. The partners first collaborated in EMODnet phase 1 (2009-2012) to deliver a prototype predictive seabed habitat map in four trial basins (Greater North Sea, Celtic Seas, Baltic, Western Mediterranean). This predictive model was named EUSeaMap (Cameron and Askew, 2011). In EMODnet Phase 2 (2012-2016), the consortium extended EUSeaMap coverage to all European regions (Populus et al, 2017).

In the new version, the spatial coverage was extended further North in order to include the Barents Sea. The spatial detail was substantially improved. This was made possible by improvements to the physical predictor variables created by the other EMODnet lots which are the input data to the EUSeaMap model. A substantial revision of the map creation process has also been carried out in order to make it more reproducible. This document describes all these modifications which have led to the elaboration of EUSeaMap 2019.

Contents

1 Introduction

EUSeaMap 2019 is the third iteration of EUSeaMap. All versions have been produced as part of the EMODnet Seabed Habitats project, which is one of several thematic lots in EMODnet. The project has brought together a European consortium of specialists in benthic ecology and seabed habitat mapping. The partners first collaborated in EMODnet phase 1 (2009-2012) to deliver a prototype predictive seabed habitat map in four trial basins (Greater North Sea, Celtic Seas, Baltic, Western Mediterranean). This predictive model was named EUSeaMap (Cameron and Askew, 2011). In EMODnet Phase 2 (2012-2016), the consortium extended EUSeaMap coverage to all European regions (Populus et al, 2017).

In the new version, the spatial coverage was extended further North in order to include the Barents Sea. The spatial detail was substantially improved. This was made possible by improvements to the physical predictor variables created by the other EMODnet lots which are the input data to the EUSeaMap model. A substantial revision of the map creation process has also been carried out in order to make it more reproducible. This document describes all these modifications which have led to the elaboration of EUSeaMap 2019.

2 Material and Methods

2.1 Material

2.1.1 Environmental variables

A series of new spatially continuous layers displaying information on the required input environmental variables were produced during Phas3 for the EUSeaMap 2019 model (Table 2.1). The majority of these data were derived from CMEMS products. Time-series gridded datasets were downloaded from the CMEMS portal and post-processed in order to calculate values at the seabed.

Table 2.1*:* Environmental variables created and compiled in Phase 3 of EMODnet Seabed Habitats for EUSeaMap 2019.

Regional Domain	Variable	Data source	Horizontal coverage	Horizontal resolution	Temporal coverage
Black Sea	Current energy	CMEMS	Full coverage	1/36x1/27 °	2016-2018
	Density	CMEMS	Full coverage	1/36x1/27 °	2011-2017
	Wave energy	Model developed by the Project	Full coverage	1/128 °	2016-2018
Mediterranean	Current energy	CMEMS	Full coverage	1/24 °	2016-2018
Atlantic	Current energy	CMEMS	Macaronesia	1/36 °	2013-2018
	Current energy	CMEMS	Iberian-Biscay-Ireland	1/36 °	2013-2018
	Temperature	CMEMS	Iberian-Biscay-Ireland	1/36 °	2013-2018
	Salinity	CMEMS	Iberian-Biscay-Ireland	1/36 °	2013-2018
	Wave energy	CMEMS	Macaronesia	1/12 °	2016-2018
	Wave energy	CMEMS	Biscay-Iberian Peninsula	1/24 °	2016-2018

Regional Domain	Variable	Data source	Horizontal coverage	Horizontal resolution	Temporal coverage
	KdPAR	MERIS	Iceland	250 m	2005-2009
	Surface PAR	MERIS	Iceland	4 km	2005-2009
Arctic	Ice cover	CMEMS	Barents	1 km	2018
	KdPAR	MERIS	Barents	250 m	2005-2009
	Surface PAR	MERIS	Barents	4 km	2005-2009

Oceanographic variables

The following section gives a brief overview of the oceanographic variables generated for inclusion into EUSeaMap 2019. Further details on how the datasets were processed are provided in Annex 1.

In the **Black Sea**, ISPRA provided a high-resolution calculation of wave energy at the sea bottom (Figure 2.1 – resolution 1/128 °, approx. 1 km) using EMODnet Bathymetry and BOLAM high-resolution meteorological data on wind (Mariani et al, 2015). Current-induced energy, temperature and salinity were derived from the CMEMS product: "Black Sea physics analysis and forecast" (CMEMS, 2018a - resolution 1/36 x 1/27 °, approx. 3 km). The density layer was calculated from temperature and salinity.

In the Mediterranean Sea, the CMEMS product, "Mediterranean Sea physics analysis and forecast" (CMEMS, 2018b - resolution 1/24 °, approx. 4.5 km), was used to produce a layer on current-induced energy.

In the Atlantic, new layers were produced for Macaronesia and the Iberian Peninsula. The CMEMS product, "Atlantic - Iberian Biscay Irish - ocean physics analysis and forecast" (CMEMS, 2018c - resolution 1/36 °, approx. 3 km), was used to generate layers on temperature, salinity and currents. Wave-induced energy layers were produced from CMEMS products: "Global ocean waves analysis and forecast" (CMEMS, 2018e - resolution 1/12 °, approx. 9 km); and "Mediterranean Sea waves hindcast" (CMEMS, 2018d - resolution 1/24 °, approx. 4.5 km). Although developed for the Mediterranean Sea, the latter also covers the Iberian Peninsula and has a better resolution than the former.

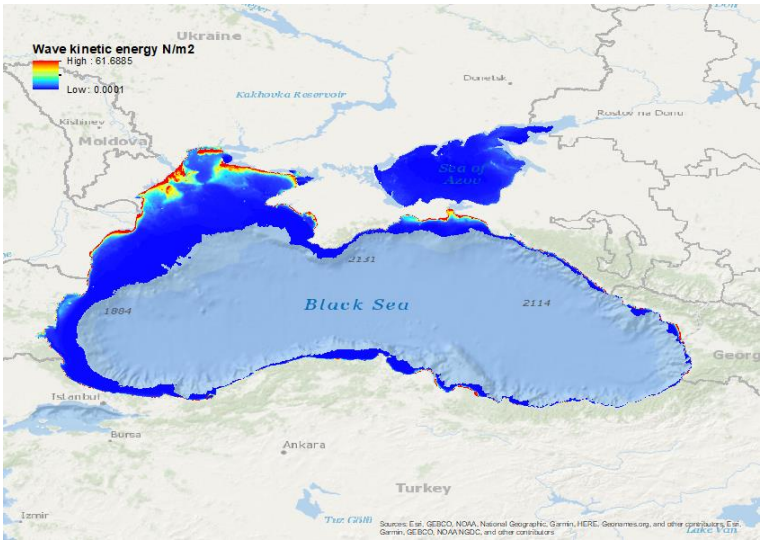

Figure 2.1: Temporally integrated percentile 90th (2016-2018) of wave kinetic energy in the Black Sea

Water transparency

Over the various phases of EMODnet, the Seabed Habitats lot has used the Saulquin et al (2013) approach to gradually develop layers on surface PAR (Photosynthetically Available Radiation) and KdPAR (attenuation coefficient of the PAR, i.e. a proxy of water transparency) from MERIS archive layers. The spatial coverage of these data was extended in EUSeaMap 2019 with the creation of new datasets for Iceland and the Barents Sea (Figure 2.2).

For each area of the following layers were produced:

- Temporally integrated means (2005-2009) of KdPAR and associated number of observations;
- Temporally integrated yearly means (2005 to 2009) of KdPAR and associated number of observations;
- Temporally integrated monthly means of KdPAR and associated number of observations.

All the provided products had a horizontal resolution of approximately 250 m.

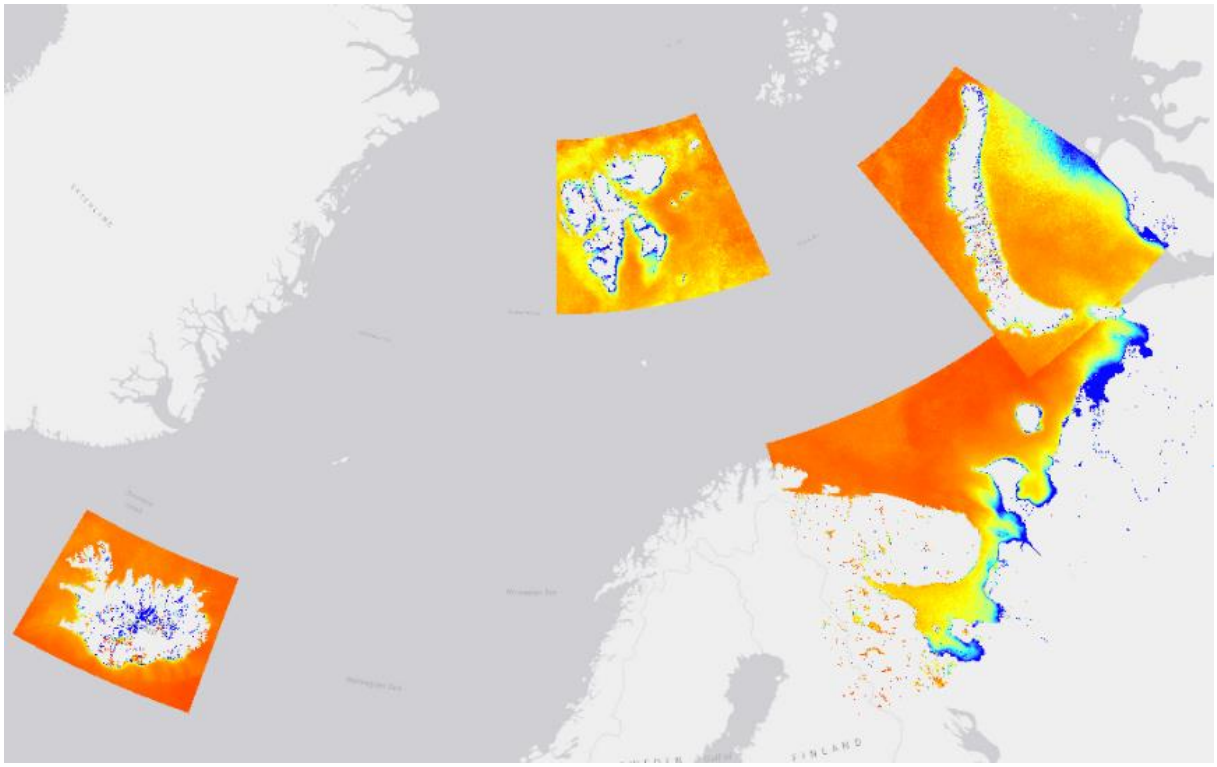

Figure 2.2: Temporally integrated means (2005-2009) of KdPAR –New areas covered for EUSeaMap 2019

Layer for sea ice concentration

The daily datasets of sea ice concentration in the Arctic were provided by the CMEMS product: "Arctic Ocean - Sea ice concentration charts - Svalbard and Greenland" (CMEMS, 2018f - approx. 1 km resolution). The data were averaged over one year (2018). The result is illustrated in figure 2.3.

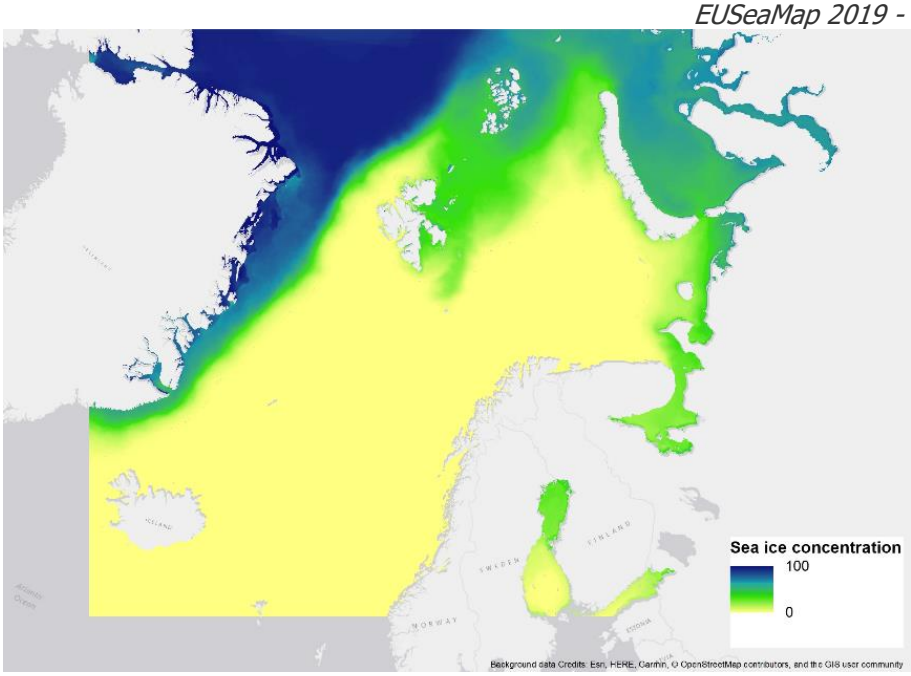

Figure 2.3: 2018 averaged ice concentation in the Arctic

Current induced energy in the Barents Sea

A 800 m resolution layer on current-induced energy was used to model current speeds in Svalbard (Figure 2.4). This layer was provided by the Norwegian Institute of Marine Research (IMR), and was derived from the dataset, "*Ocean and sea ice circulation model results from Svalbard area",* (Albretsen et al, 2017).

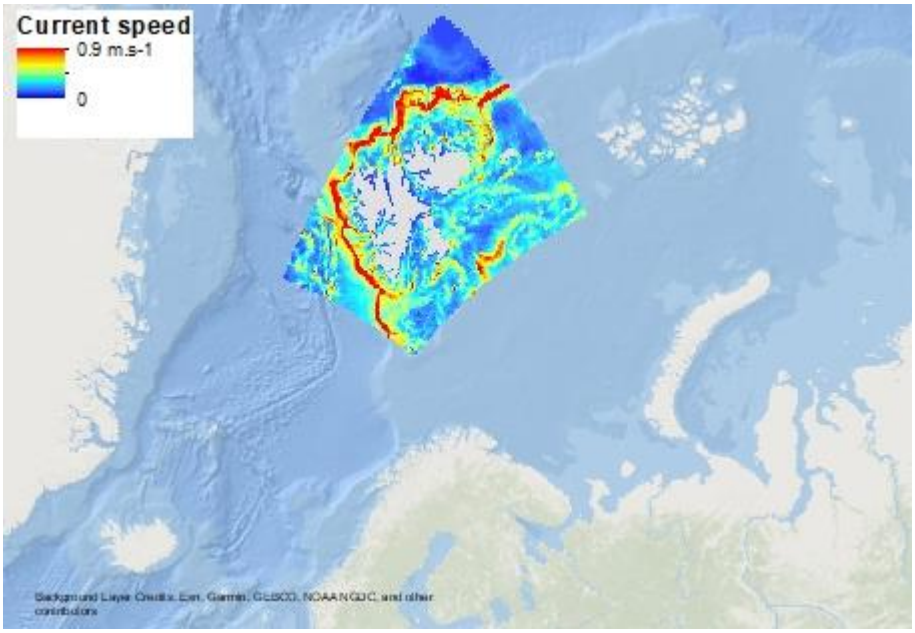

Figure 2.4: Yearly-averaged current speed (90th precentile) in Svalbard

2.1.2 Seabed Substrate

Seabed substrate data are one of the most important input data layers used in the generation of EUSeaMap. Seabed types are classified according to a modified version of the Folk classification system displaying 7 classes. The data were standardised and merged into a single vector file (Figure 2.5). The data were collated from the following archives:

- EMODnet Geology maps (1:1M, 1:250k, 1:100k and 1:50k scale);
- MeshAtlantic Project map in the Azores (Mata Chacón et al, 2013);
- A map compiled as part of ur-EMODnet Seabed Habitats in the western Mediterranean (Cameron and Askew, 2011);
- Multisource Posidonia meadows (dead and alive);
- A non-published map of hard substratum in the Mediterranean;
- A non-published map off Bulgaria, produced by the EMODnet Seabed habitats' partner IO-BAS;
- A modelled rock layer in Norway (referred to as "Proxy for rock in Norway" in Populus et al, 2017);
- A layer of predicted outcrops or subcrops of rock in UK shelf seabed (JNCC, 2019).

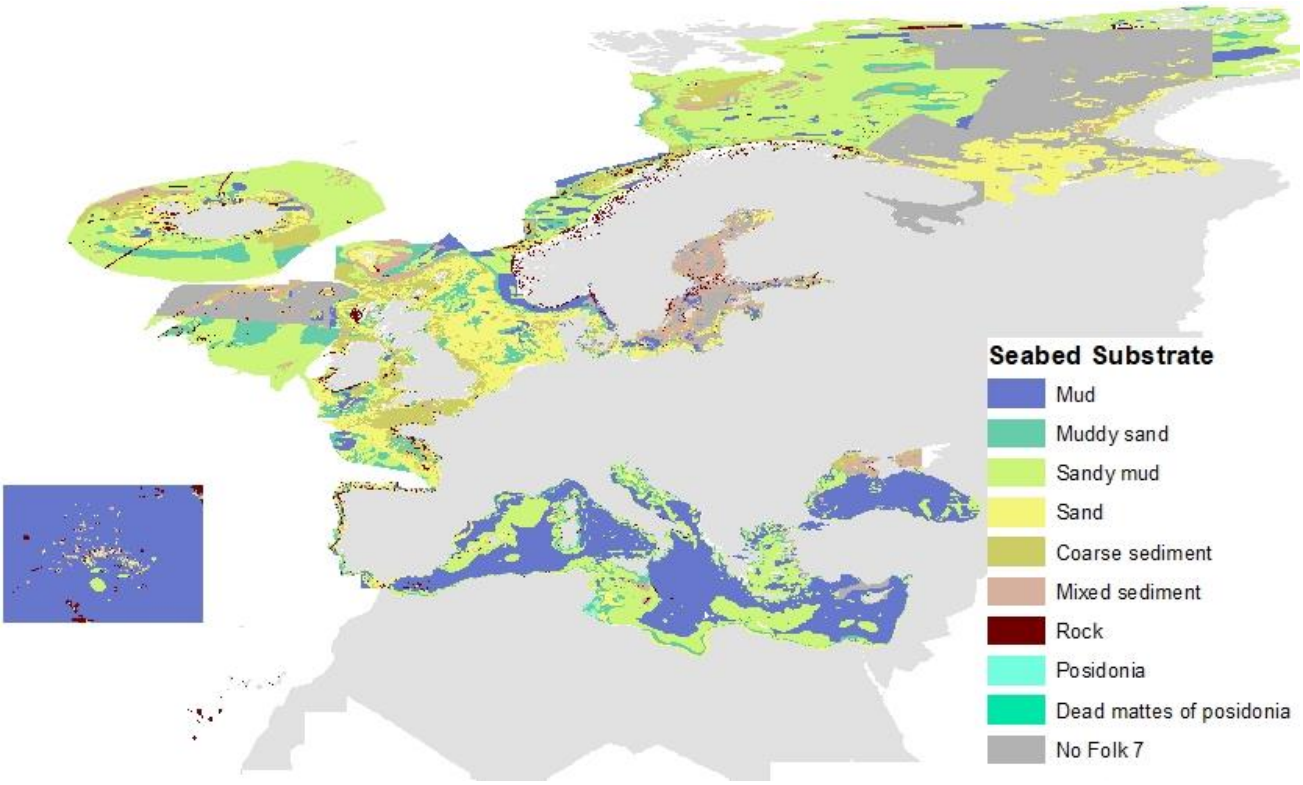

Figure 2.5: Compilation of seabed substrate types

In 2019 the EMODnet Geology Lot made seabed substrate data available at two additional scales: 1:100K and 1:50K. Existing maps at the scale 1:1M and 1:250K were not updated. EUSeaMap 2019 incorporated the new, higher resolution seabed substrate data. An illustration of the spatial extent of the seabed substrate data at these larger scales is shown in Figure 2.6.

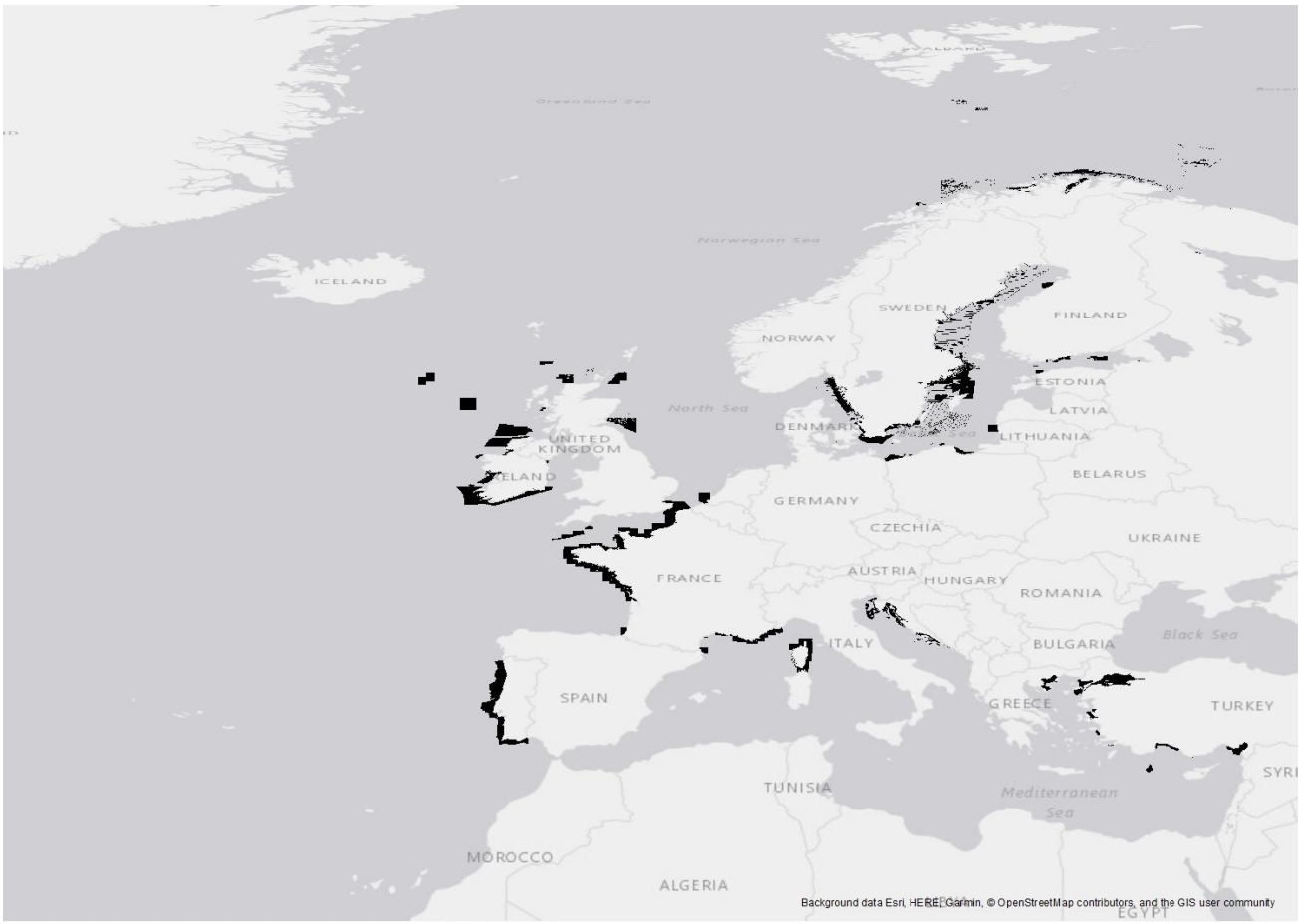

Figure 2.6: Footprint of seabed substrate data at higher resolutions included in EUSeaMap 2019

2.1.3 Bathymetry

Bathymetry is used to calculate biological zones in EUSeaMap. The EMODnet Bathymetry Lot released an updated DTM in 2018 (Figure 2.7, EMODnet Bathymetry Consortium, 2018). The resolution of the new version is 100 m and constitutes a significant update to the previous version which had a resolution of 250 m.

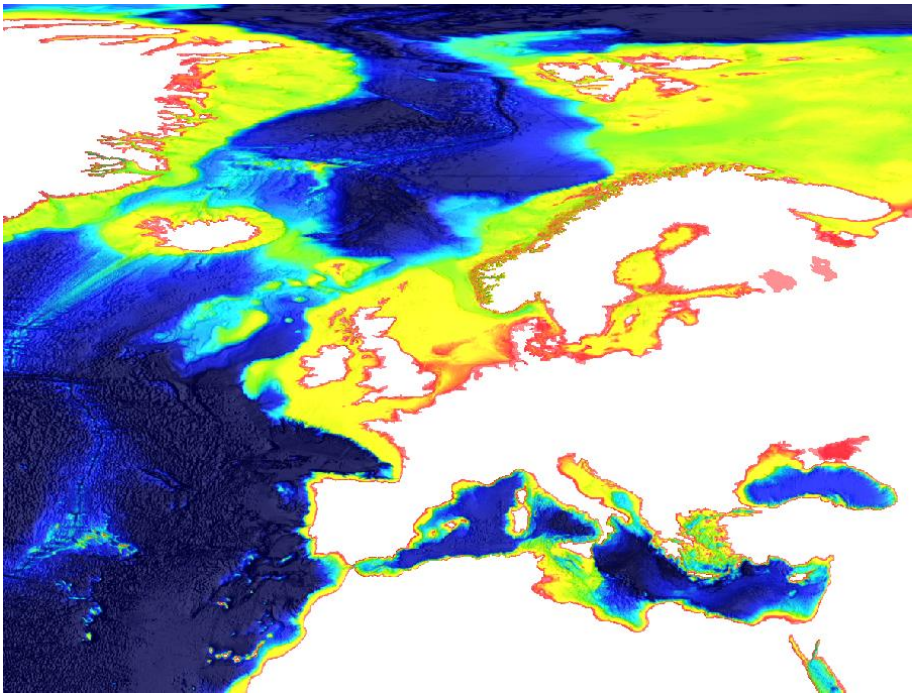

Figure 2.7: EMODnet Bathymetry DTM, version 2018

2.2 Methods

2.2.1 A revised GIS workflow

In previous phases of EMODnet, a commercial software was used to generate EUSeaMap. A key objective of phase 3 was to develop a new GIS workflow that would be sound, repeatable and transferrable across basins, and to implement this workflow in a tool based on open-source technologies.

The GIS workflow is presented as a schematic in Figure 2.8. In step 1 each habitat descriptor layer (i.e. input data such as biological zone, oxygen regime, energy regime, etc) is produced as a raster before being converted to a vector polygon layer in step 2. All habitat descriptor layers, and the seabed substrate layer (referred to as "preclassified layer" in Figure 2.8), are overlaid in step 3 to create the habitat layer. Once all the data are combined, a lookup table that correlates numerical habitat codes with various defined habitat classes (e.g. EUNIS, MSFD broad habitat types) is joined to the habitat layer in step 4.

The qualitative habitat descriptor layers, and their associated measures of confidence, were derived from the input quantitative environmental variable layers using map algebra (Coltman et al, 2008; Vasquez et al, 2015; Populus et al, 2017) in the R package *raster*.

Overlaying the data was the most challenging step. A raster-based approach was used to overlay the habitat descriptor layers in EUSeaMap 2016. This approach requires working at a fixed resolution. In order to allow multi-scale data, such as the seabed substrate data, to be incorporated into the map-making process, the existing workflow had to be modified. This modification involved the final overlay of the habitat descriptor

layers to be in vector mode. Several options were studied for the overlay, namely ARCGIS™, QGIS, GRASS and two R packages: rgeos and raster (see Annex 4 for a full report of the study). The main findings of this study concluded that ArcGIS™ and GRASS were the most fit-for-purpose. With a view to using an open-source solution, we initially developed an R script performing the overlay using GRASS. However, this option proved to be impractical on account of the length of time it took to run the script, typically several hours. In contrast, ARCGIS™ required only a few minutes and was therefore the preferred option.

Taking into consideration all of the aforementioned reasons, the GIS workflow was implemented using R scripts for steps 1 and 2, and an ArcGIS™ model builder for steps 3 and 4.

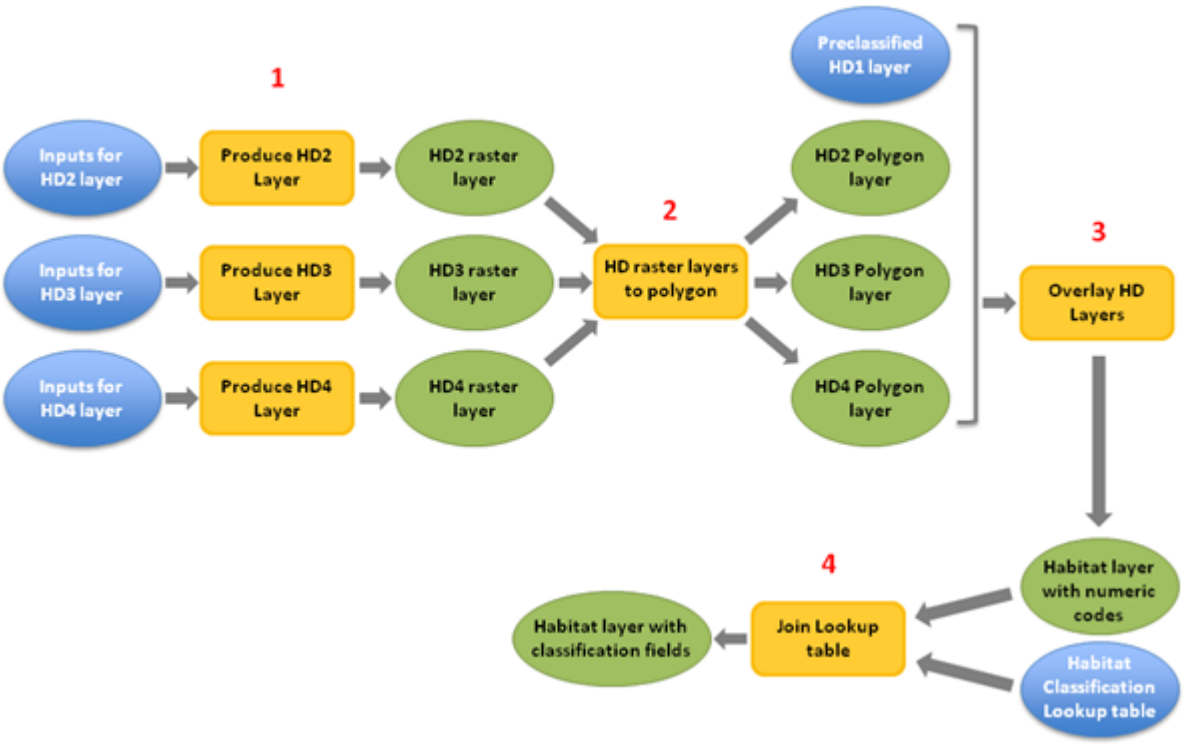

Figure 2.8: The EUSeaMap GIS workflow. All habitat descriptors (HD) layers are;1) produced as rasters; 2) converted to polygon; 3) overlaid to create the habitat layer. After the overlay, a lookup table that correlates numerical habitat codes with various habitat classes is joined to the habitat layer (4).

2.2.2 Habitat classifications

The habitat map was classified into three classification systems to facilitate a wide range of applications:

1. EUNIS habitat classification system version 2007-11 (levels 3 and 4) - This is the standard classification system for Europe. However, it lacks definition in the deep-sea and does not describe the habitats in the Arctic, Barents Sea, and Baltic Sea in sufficient detail. EUNIS version 2007-11 was deemed unsuitable to describe habitats in the Black Sea, therefore, a tailored classification was created for EUSeaMap 2016 (Populus et al, 2017).
2. MSFD benthic broad habitat types - This is a coarse scale classification system defined in COMMISSION DECISION (EU) 2017/848. The correlation table proposed by Manca et al (2017) was used to translate EUNIS habitats into these habitat types.
3. Full-detail classification - This incorporates EUNIS classes, and additional, detailed classes which cannot be adequately described using higher levels of EUNIS, e.g. habitats in the Black Sea, ice-cover in the Barents Sea and water masses in the deep-sea.

2.2.3 Thresholds

Methods previously developed as part of EUSeaMap 2016 were used to calculate threshold values. These values enable physical data to be classified into discrete habitat descriptor classes (Populus et al, 2017). Using these methods, threshold values were identified by analysing the overlap between marine communities and habitat descriptor classes. In addition to providing a means for classifying habitat descriptor classes, the methods can also be applied to calculate the probability of occurrence of the habitat descriptor classes at all locations (pixels), a measure that is used at a later stage as an input for confidence assessment (see step 2 in the next section).

2.2.4 Confidence

The method to assess the confidence of EUSeaMap, fully described in Populus et al (2017), is a raster-based assessment where each pixel is assessed on the basis of the following:

1. The confidence in the values of continuous variables. This is measured according to various specific criteria (e.g. the "wave-induced energy" variable confidence is based on the spatial resolution; the kdPAR variable confidence is based on the number of satellite image per grid cell).
2. The confidence in classification of habitat descriptors. For each habitat descriptor class boundary, [0-1] values of the habitat descriptor class presence probability are calculated via fuzzy laws or a GLM equation (derived from biology observations).

The raster layers obtained from these two assessments are combined. The result displays qualitative measures of confidence: high, moderate and low.

As mentioned in section 2.1.2, the seabed substrate layer is a compilation of several data sources, the predominant one being EMODnet Geology. The original confidence scores for each data source and their translation into qualitative measures of confidence for EUSeaMap 2019 are presented in Table 2.2.

Table 2.2: Substrate Confidence - Translation from the various confidence assessments associated with substrate datasets used in EUSeaMap into high, medium and low confidence.

	EMODnet Geology maps	MeshAtlantic Azores	ur-ESH west Med.	Posidonia meadows	hard bottoms in the Med.	off Bulgaria	rock in Norway	rock in UK
High	3,4		>60	Presence	Presence			3,4
Medium	2,1		<60			Presence		2,1
Low	0, no data	Presence					Presence	0, no data

EMODnet Bathymetry provides a confidence assessment of the data used to construct its DTM. The assessment methodology was entirely revised in 2018 (EMODnet Bathymetry Consortium, 2019). Each cell is assigned a confidence value in the interval 0-100. Cut-off values of 40 and 70, as recommended by the authors, were used to classify the areas on the map into low, moderate and high. The qualitative confidence values for the seabed substrate and bathymetry layers are illustrated in Figure 2.9.

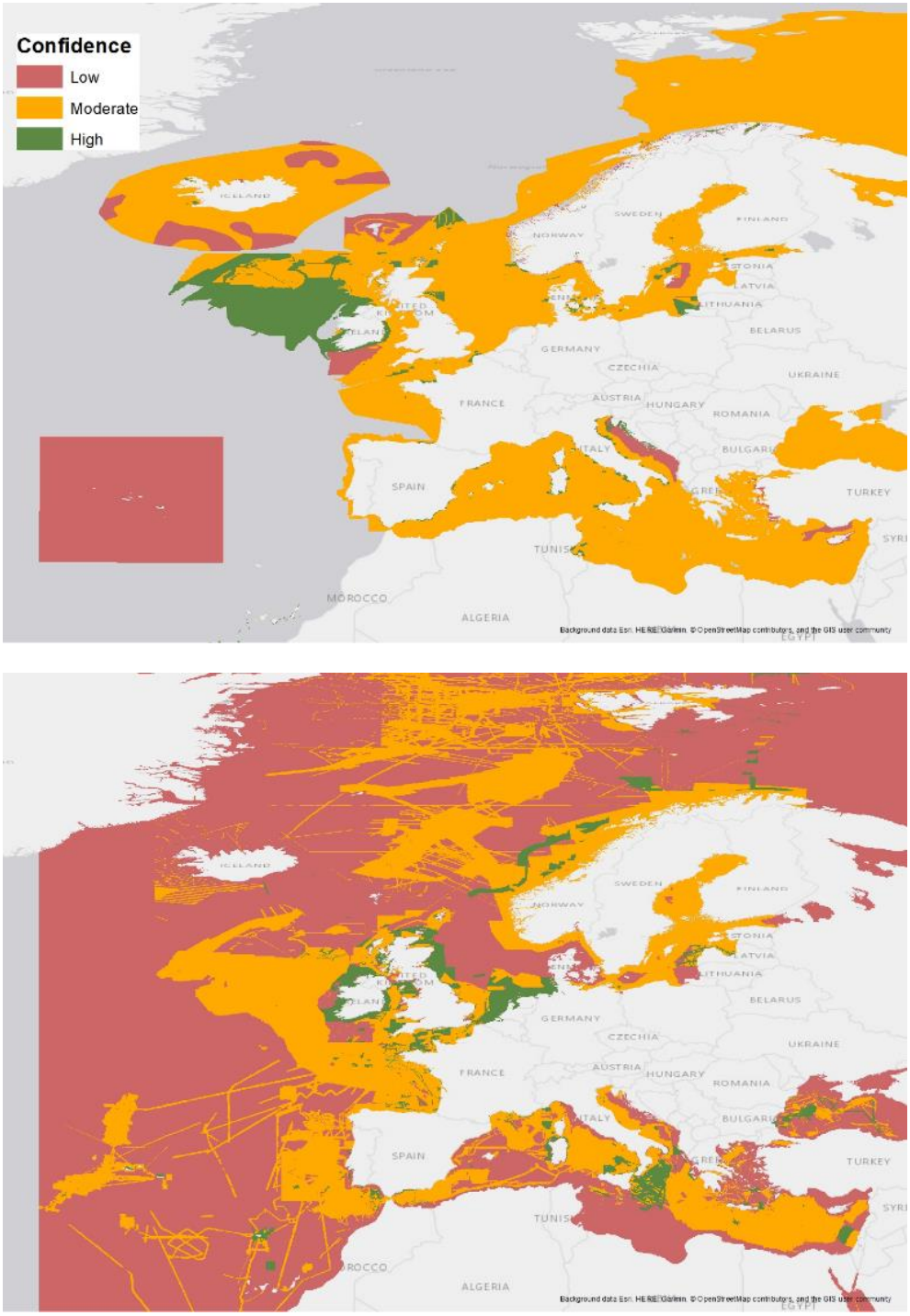

Figure 2.9: Confidence map for seabed substrate (top) and bathymetry (bottom)

3 Results

3.1 EUNIS classification

The updated version of EUSeaMap (2019) classified according to EUNIS is presented in Annex 2. The following subsections provide a brief summary of the modifications made in each marine region.

3.1.1 Black Sea

3.1.1.1 EUNIS applicability

EUNIS classes were deemed not applicable in the Black Sea (Populus et al, 2017) in EUSeaMap 2016. Consequently, a bespoke "EUNIS-like" classification was defined. This habitat classification has been significantly modified (see further detail in Annex 4) in EUSeaMap 2019.

3.1.1.2 Threshold update

The threshold for the infralittoral/circalittoral boundary for soft bottoms were revised locally along the Bulgarian coast (changed to -13m, in comparison to -20m elsewhere) in order to better reflect the sheltered nature of that section of coastline.

Another major update were the thresholds which enabled the classification of the seabed into "oxic", "suboxic" and "anoxic". The experts of the consortium agreed on values of 15.9 kg.m^{-3} and 16.4 kg.m^{-3}.

3.1.1.3 Habitat map

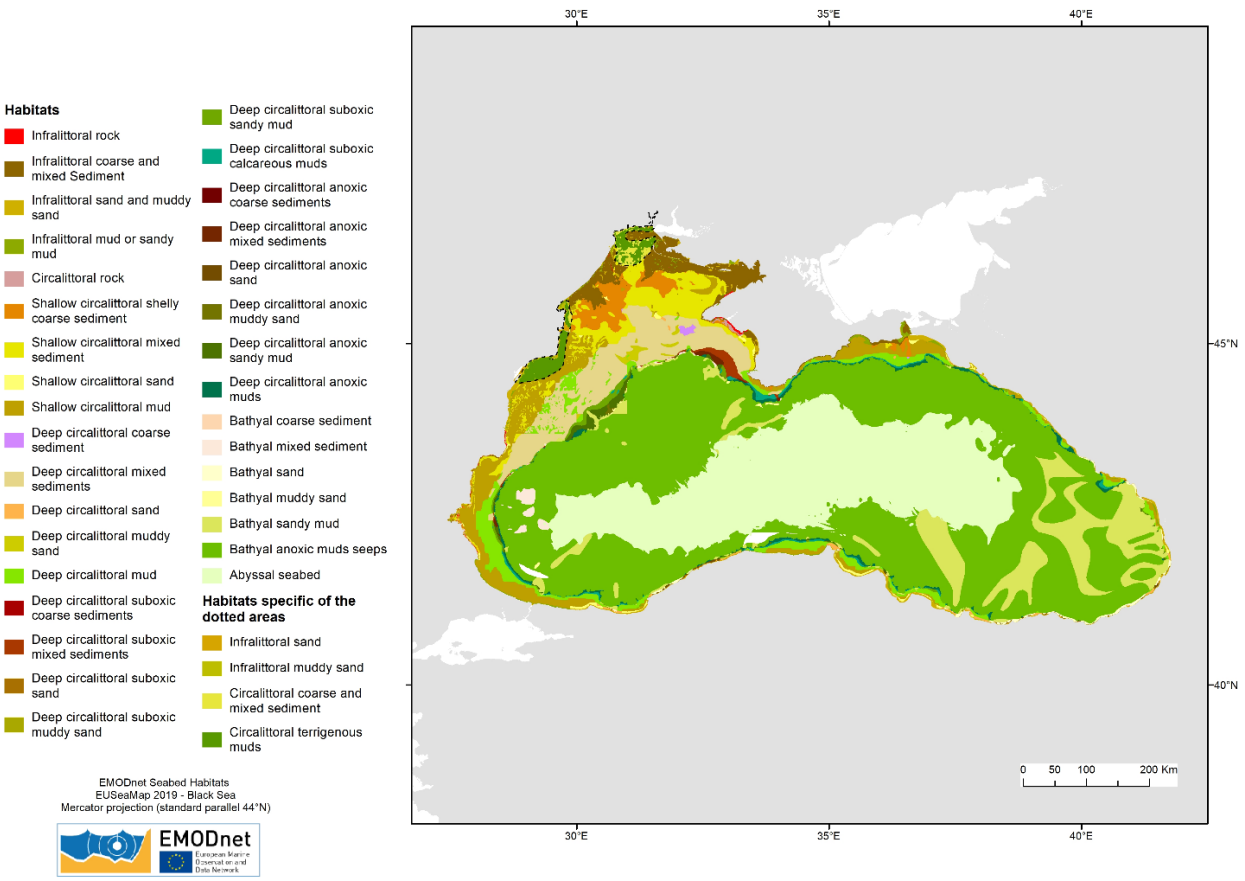

Figure 3.1: habitat map in the Black Sea

3.1.2 Mediterranean Sea

3.1.2.1 EUNIS applicability

Levels 3 and 4 of EUNIS version 2007-11 are appropriate for describing the variation in physical seabed habitat types. Occurrences of the seagrass species *Posidonia oceanica* and *Cymodocea nodosa* were were included in EUSeaMap 2016. It was decided that the habitat-forming species that cover and replace the underlying substrate as a structuring factor should only be included in EUSeaMap 2019. *Posidonia oceanica* meet this requirement while *Cymodocea nodosa* does not. As a result, only *Posidonia oceanica* coverage were included in version 2019.

3.1.2.2 Threshold update

Due to the major update of the DTM produced by EMODnet Bathymetry, boundaries based on severe slope changes were revised. These include the boundaries between shelf and bathyal and between bathyal and abyssal.

3.1.2.3 Habitat map

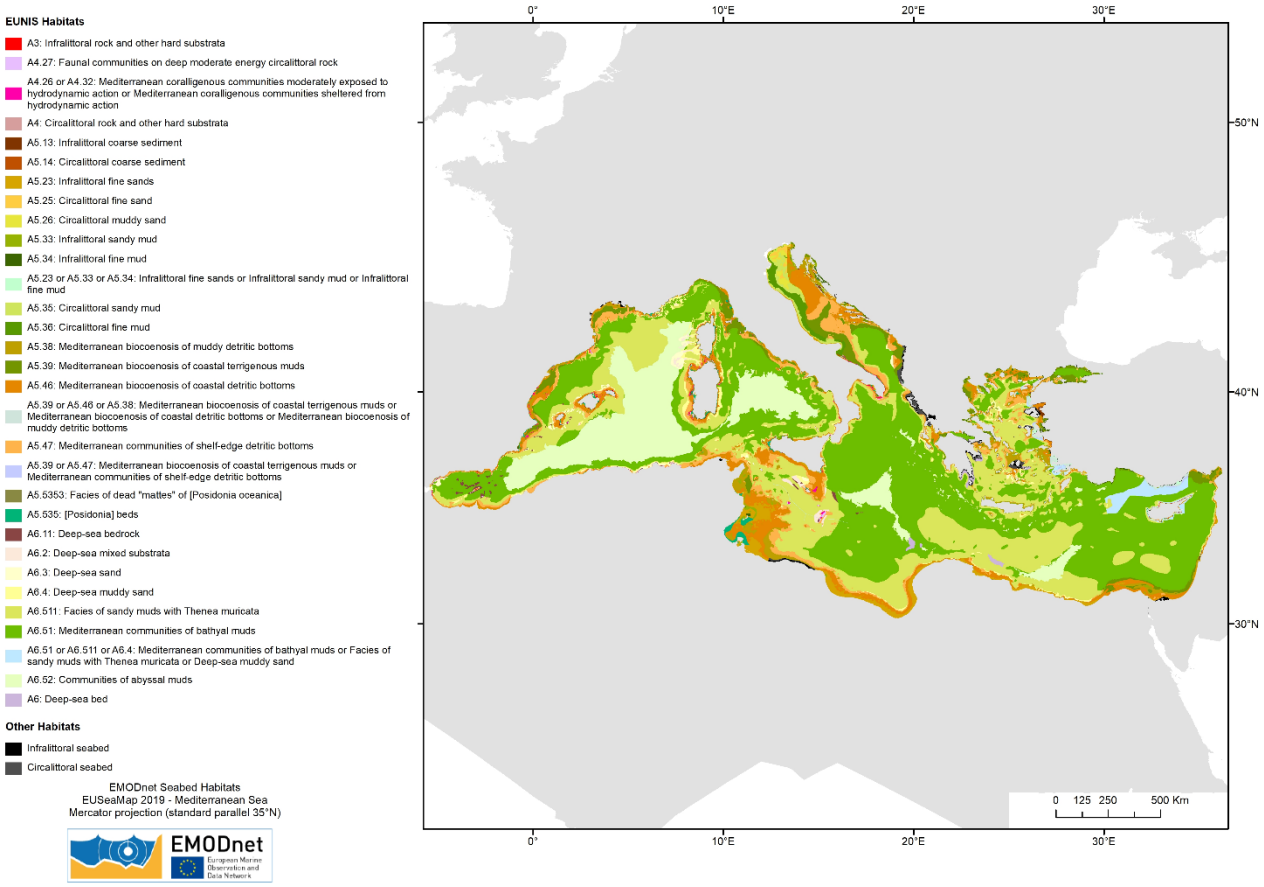

Figure 3.2: EUNIS habitat map in the Mediterranean Sea

3.1.3 Baltic Sea

3.1.3.1 EUNIS applicability

Levels 3 and 4 of EUNIS version 2007-11 are suitable to some extent in describing the variation in physical seabed habitat types. In addition to the standard EUNIS classification, an alternative classification was also mapped, which further divides each EUNIS class into four sub-classes depending on the salinity regime: oligohaline, mesohaline, polyhaline and marine.

3.1.3.2 Threshold update

Thresholds were not updated. However, in order to define the infralittoral/circalittoral boundary in the mesohaline waters along the Swedish and Finnish coast, data on the spatial distribution of the photic zone, produced by fine-scale national studies (Hammar et al, 2018; Lappalainen et al, 2019), were incorporated. These data were provided in the form of a categorical photic/non-photic dataset. An improved dataset of salinity for part of the region in the Finnish Exclusive Economic Zone, owned by SYKE, was incorporated into the salinity layer.

3.1.3.3 Habitat map

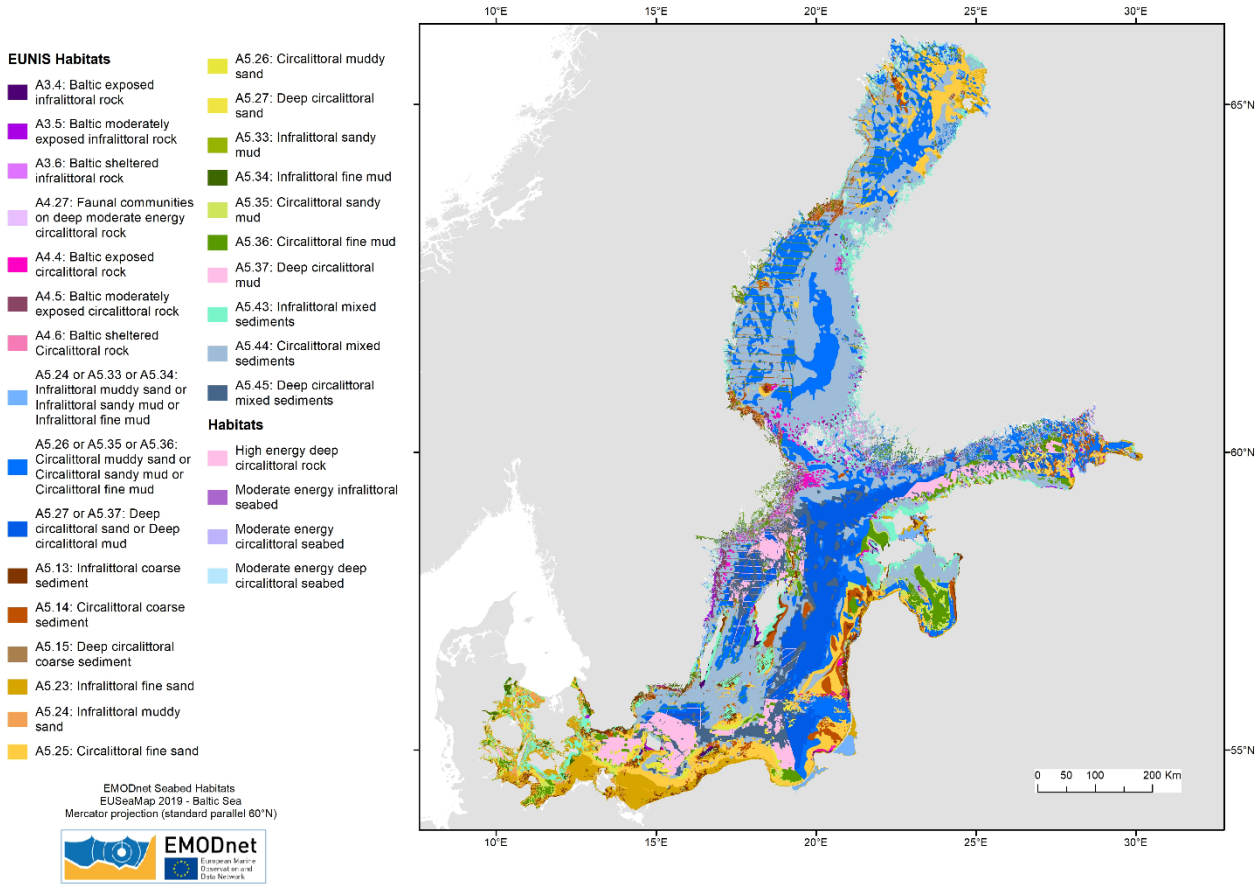

Figure 3.3: EUNIS habitat map in the Baltic Sea

3.1.4 North East Atlantic Ocean

3.1.4.1 EUNIS applicability

Levels 3 and 4 of EUNIS version 2007-11 are suitable for describing the variation in physical seabed habitat types in most part of the Regional Seas in the Atlantic. Despite the limitations of EUNIS in the most northern parts of Europe, the classification was used in areas of the Barents Sea that are not covered by ice.

3.1.4.2 Threshold update

The new wave energy layer produced by CMEMS for the Bay of Biscay and the Iberian Peninsula has brought substantial improvement in terms of spatial resolution to Northern Spain and the Straits of Gibraltar. The threshold analysis led to values of 40 $N.m^{-2}$ for the low/moderate energy boundary, and 80 $N.m^{-2}$ for the moderate/high energy boundary. In Iceland and the Barents Sea, the PAR at seabed threshold value that is used in other areas of the Atlantic for differentiating between infralittoral and circalittoral (i.e. 0.7 $mol.pho.m^{-2}.d^{-1}$, Populus et al, 2017) was used.

A threshold of 20% ice concentration was used as the demarcation between open sea and sea ice in the Barents Sea.

3.1.4.3 Habitat map

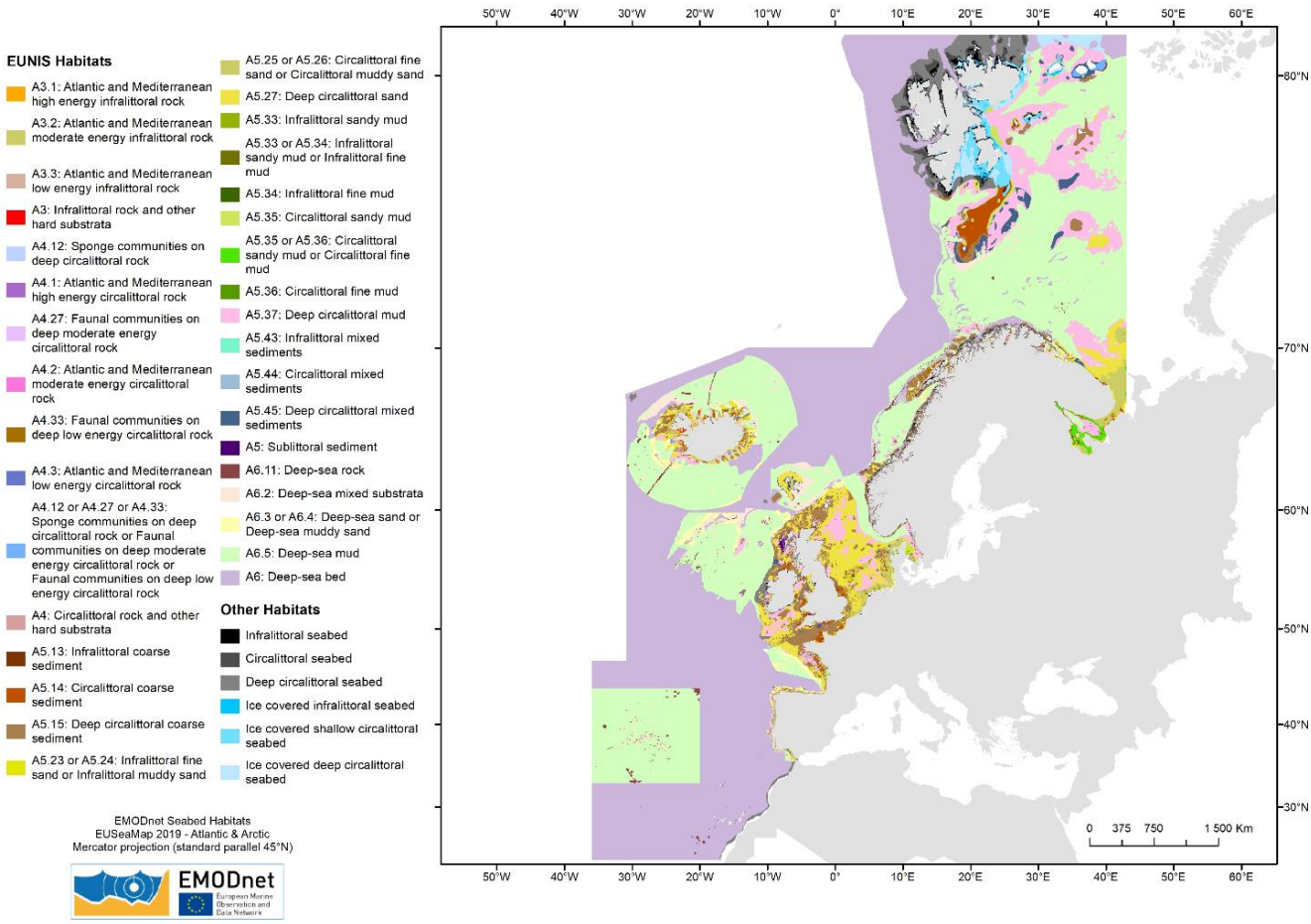

Figure 3.4: EUNIS habitat map in the North East Atlantic

3.2 MSFD broad habitat types

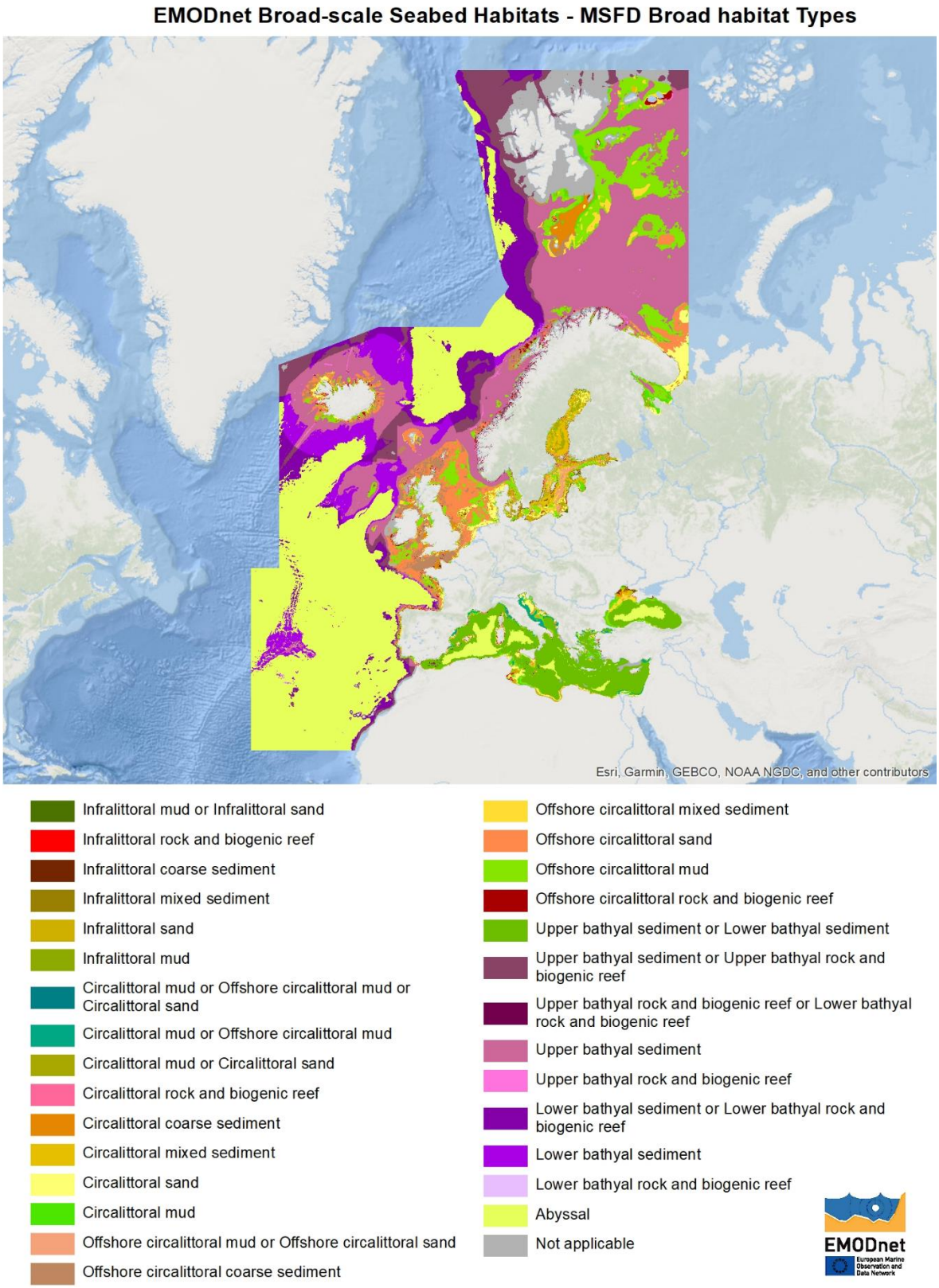

Figure 3.5: EUSeaMap in the MSFD broad habitat classification

3.3 Discussion

As a result of the new, vector-based approach, EUSeaMap 2019 is now multi-scale. Previous versions were at a fixed scale of around 1:1M. Therefore, EUSeaMap 2019 is much more detailed in areas where the seabed substrate data is more detailed, as illustrated in the two examples shown in Figure 3.6.

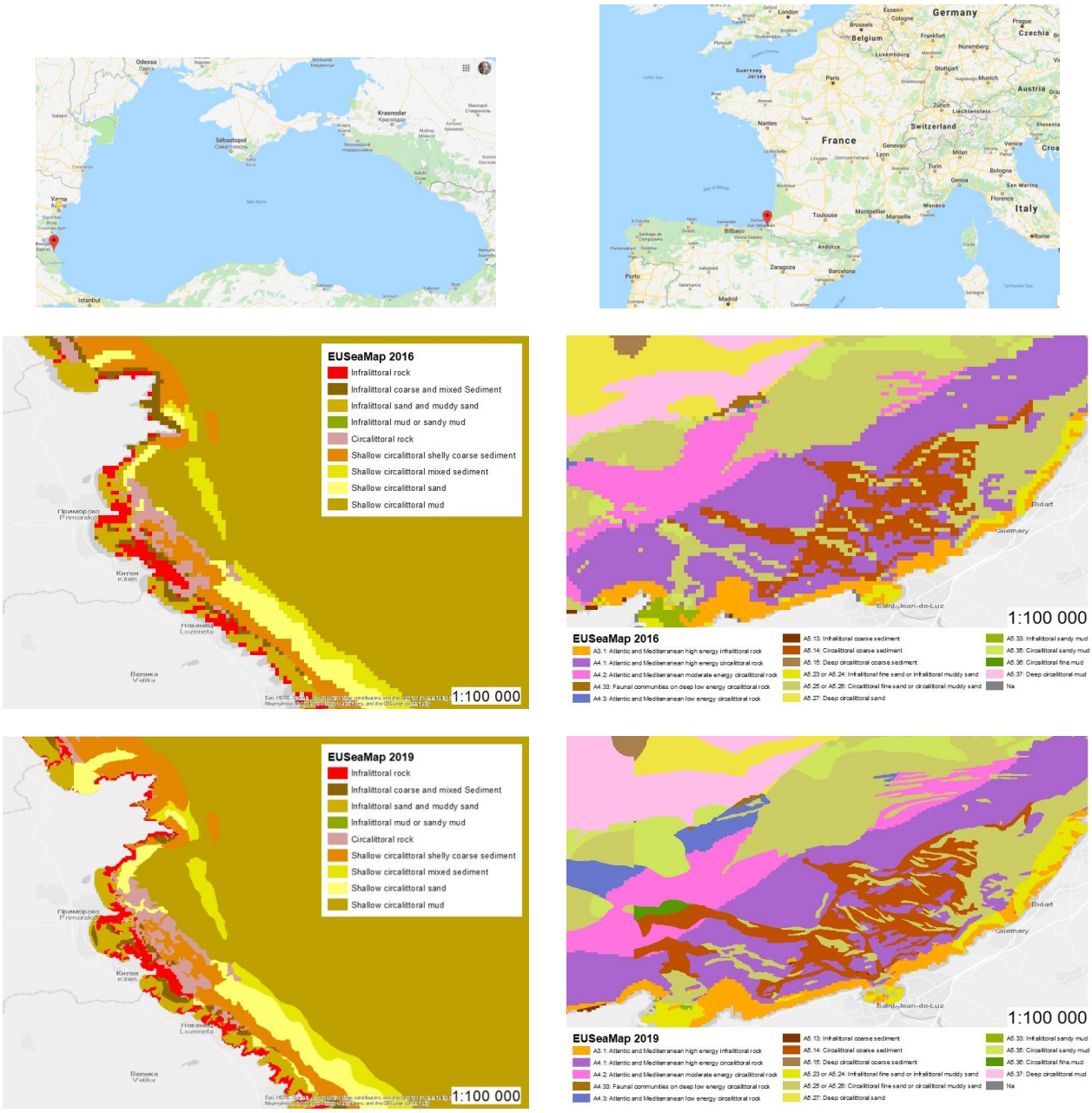

Figure 3.6: EUSeaMap 2019 (bottom) vs EUSeaMap 2016 (middle) in two local areas in Bulgaria (left) and France (right)

Due to the integration of more detailed seabed substrate data covering large areas along the European coasts (see Figure 2.6) and higher resolution bathymetric data (100 m compared to 250 m in the previous version), the spatial distribution of the different habitat types described in EUSeaMap was likely to change in a significant way. Annex 5 provides a comparison across MSFD regions or subregions between the two versions of EUSeaMap in terms of spatial coverage for i) the biological zones; ii) the seabed substrate; and iii) the MSFD broad habitat types.

Due to the increase in the spatial resolution of the DTM, there was a slight change in the spatial distribution of biological zones (Annex 5, Tables 12.2 and 12.3). In tidal regions, the infralittoral footprint has slightly decreased, while in non-tidal regions (Mediterranean, Black Sea, Baltic Sea) the infralittoral footprint has increased. In tidal regions, the new version of the EMODnet Bathymetry DTM uses the LAT (Lowest Astronomical Tide) as the hydrographic zero, whereas the HAT (Highest Astronomical Tide) was used in the previous version for some regions. This change is obvious in areas subject to high tides, e.g. Figure 3.7. As a result, the infralittoral, the upper limit of which is the zero value provided by the DTM, was slightly overestimated in EUSeaMap 2016.

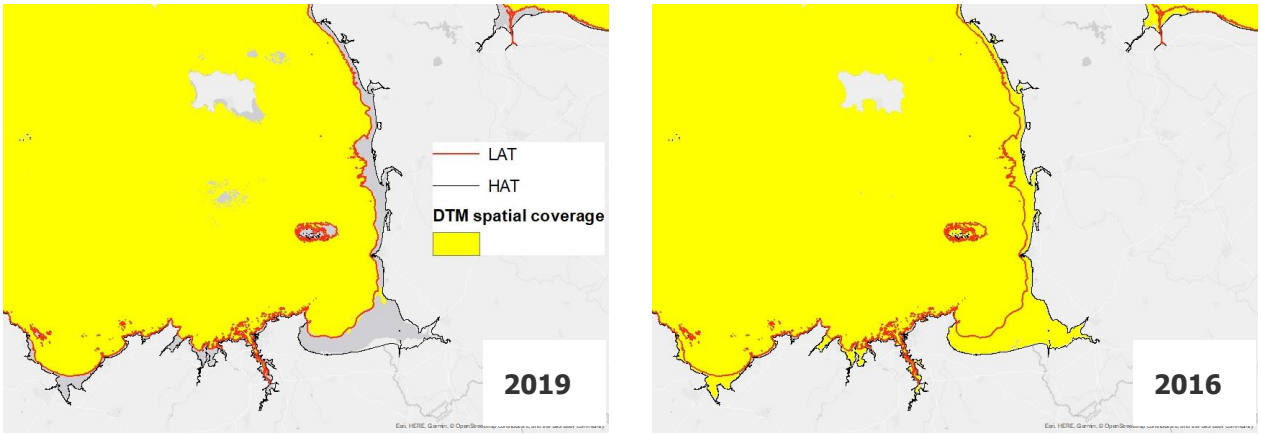

Figure 3.7: Spatial coverage (yellow) of the 2019 DTM (left) vs the 2016 DTM (right) in an area subject to high tides (Mont-Saint-Michel, France). In version 2016, the DTM reaches the coast because the HAT was used as the DTM zero value, whereas in version 2019, the LAT has been used as the DTM zero value.

In non-tidal regions, a consequence of the increased resolution of the DTM is that more pixels are coming closer to the coast, resulting in greater spatial coverage of the DTM all along the coasts of these regions, and therefore an increase in the infralittoral footprint.

The changes in the spatial distribution of seabed substrate types are more significant (Annex 5, Tables 12.5 and 12.6). These are observed in areas where the new higher resolution data have been included in EUSeaMap, e.g. in the Bay of Biscay and the Iberian Coast (+56% coarse substrate, -38% mixed sediment), in the Celtic Seas (-48% Rock) and in the Black Sea (+17% rock, +36% mixed sediment, -29% sand).

As a result, changes in the spatial distribution of MSFD broad habitat types (Annex 5, Tables 12.8 and 12.9) correspond to areas where new seabed substrate have been included.

4 Conclusion and Perspectives

4.1 Conclusion

By including new areas, namely the Barents Sea and Iceland, EUSeaMap now covers 87% of the European regions that are considered by the dataset 'Europe's seas' published by the EEA[1], compared to 79% in version 2016. This is a significant extension.

The biggest challenge in the creation of EUSeaMap 2019 was to meet the tender specification for phase 3, which required the inclusion of maps with "as fine detail as the underlying data permit". The resulting map succeeded in displaying habitats at the best possible spatial resolution. This was achievable due to the development of a new methodology specifically developed to combine all of the input, multi-resolutional data.

The inclusion of more accurate seabed substrate data, a DTM with better resolution, and additional environmental layers have contributed to significant improvements to EUSeaMap in the following areas: Greater North Sea (including the Kattegat and the English Channel); the Bay of Biscay and the Iberian Coast; and in parts of the Baltic and the Mediterranean Sea.

Improvements to the level of detail on habitats in Black Sea are as a result of a review conducted in 2016, which led to the development of a more appropriate habitat classification. There is still some progress to be made in this region. However, this is beyond the scope of EUSeaMap, as the issue is due to the lack of available knowledge on the seabed in this region and therefore an absence of data. In particular, data on the spatial distribution of shelly sediments is poor, which has implications for management of these areas in the infralittoral and circalittoral which host important marine communities. The spatial coverage of bathymetric data is also an issue in this region, especially in shallow waters. As a result, the spatial distribution of the infralittoral zone is not always accurately portrayed.

Version 2019 of EUSeaMap for the first time covers the Barents Sea. The EUNIS classification is not commonly applied in habitat mapping surveys in Norwegian waters because the habitats within EUNIS do not accurately reflect the habitats present on the seafloor. It should be noted that unless further work is done to develop the EUNIS classification to better reflect the habitats present in these areas, there will be limitations in the quality of the map that can be produced.

4.2 Perspectives

Short-term perspectives

It is expected that more seabed substrate data will become available in the future. Therefore, EUSeaMap will have to be updated on a regular basis, possibly every two years. At some point, a decision will have to be made on the required level of detail of the seabed substrate maps that are to be integrated into EUSeaMap e.g. is it appropriate to include a fine-scale, detailed map, covering a small area, into a broad-scale map? It could be argued that these fine-scale maps create the illusion that the seabed is much more diverse than the surrounding seabed.

An update to the EUNIS classification (EUNIS 2019) has recently been published. It is a major update, that is meant to better reflect regional particularities. Among other novelties, it now includes the HELCOM HUB classfication in the Baltic. EUSeaMap will then have to be translated into that new version that will probably be the new standard in European waters in the future. In the new version, biogenic habitats (e.g. worm reefs, biogenic peat bottoms, mussel beds, coralligenous platforms) are identified at the highest hierarchical levels of

[1] https://www.eea.europa.eu/data-and-maps/data/europe-seas

the classification. Regarding these habitats, the integration of existing polygons from surveys into EUSeaMap (as has been done for *Posidonia oceanica)* will need to be formalised. There are pros and cons to this scenario e.g. there are very limited data on the spatial distribution of some of these habitats, which poses the question on whether or not to include these habitats into EUSeaMap.

Beyond EUSeaMap

For the purposes of coherence in habitat description across European waters, initiatives for the development of EUNIS-compatible seabed habitat classification in northern regions and in the Black Sea are strongly recommended. Regarding the latter, the classification that EMODnet Seabed Habitats has developed, with Romanian and Bulgarian seabed habitat experts, may be a good starting point.

As previously stated, EUSeaMap can be improved on a regularly basis as new datasets on seabed substrate distribution are released. In the future, consideration should be given to a new suite of data products that can inform stakeholders, such as species distribution models (SDMs). SDMs have been proven to accurately predict the spatial distribution of some key habitat-forming species (e.g. Kelly et al, 2011; Gorman et al, 2012; Virtanen et al, 2018; for a review see Virtanen et al, 2019). The prerequisite for a large, operational species distribution modelling (SDM) program in Europe is the availability of oceanographic data throughout Europe at the appropriate resolution for SDM, which we believe to be somewhere in the region of 500 m.

5 Data access

The latest, updated version of EUSeaMap (2019) and all data used as inputs into its generation including habitat descriptor maps (biological zone, energy levels, salinity regimes, etc.), confidence maps and environmental data layers, can be viewed and downloaded from the EMODnet Seabed Habitats thematic portal: https://www.emodnet-seabedhabitats.eu/

6 Acknowledgements

The project would like to acknowledge the valuable contributions of many individuals and organisations:

- DG-MARE funded the contract with the Seabed Habitat Lot
- Our colleagues working on other EMODnet lots, namely, Bathymetry, Geology, Physics and Biology. In particular, our thanks go to Susanna Kihlman and Aarno Kotilainen (GTK) of the Geology group did their utmost to deliver excellent seabed substrate maps ahead of the official release, and also to Benoit Loubrieu (Ifremer) and Thierry Schmitt (SHOM), for kindly addressing bathymetry confidence under our request. Antonio Novellino (EMODnet Physics) provided us with a layer on Ice concentration.
- Jon Albretsen (IMR), Genoveva Gonzalez-Mirelis (IMR), Margaret Dolan (NGU) and Pål Buhl-Mortensen (IMR) kindly provided expertise and datasets for the Barents Sea.
- Dimitar Berov (Institute of Biodiversity and Ecosystem Research, Bulgaria) for providing us with point observation data of infralittoral/circalittoral hard bottoms communities in the Black Sea and for sharing his expertise in that field.

7 References

Albretsen, J., Hattermann, T., Sundfjord, A., 2017. Ocean and sea ice circulation model results from Svalbard area (ROMS) [Data set]. Norwegian Polar Institute. https://doi.org/10.21334/npolar.2017.2f52acd2

Cameron, A. and Askew, N. (eds.), 2011. EUSeaMap - Preparatory Action for development and assessment of a European broad-scale seabed habitat map final report. https://www.emodnet-seabedhabitats.eu/media/1593/20110228_finalreport_euseamap_v28.pdf

CMEMS, 2018a – Product user manual for the Black Sea Physical Analysis and Forecast Product - BLKSEA_ANALYSIS_FORECAST_PHYS_007_001. Issue 2.1. https://resources.marine.copernicus.eu/documents/PUM/CMEMS-BS-PUM-007-001.pdf

CMEMS, 2018b – Product user manual for Mediterranean Sea Physical Analysis and Forecasting Product - MEDSEA_ANALYSIS_FORECAST_PHY_006_013. Issue 1.1. https://resources.marine.copernicus.eu/documents/PUM/CMEMS-MED-PUM-006-013.pdf

CMEMS, 2018c – Product user manual for Atlantic -Iberian Biscay Irish- Ocean Physics Analysis and Forecast Product - IBI_ANALYSIS_FORECAST_PHYS_005_001. Issue 6.0. https://resources.marine.copernicus.eu/documents/PUM/CMEMS-IBI-PUM-005-001.pdf

CMEMS, 2018d – Product user manual for Mediterranean Sea Waves Hindcast Product - MEDSEA_HINDCAST_WAV_006_012. Issue 1.1. https://resources.marine.copernicus.eu/documents/PUM/CMEMS-MED-PUM-006-012.pdf

CMEMS, 2018e – Product user manual for GLOBAL Ocean Waves Analysis and Forecasting Product- GLOBAL_ANALYSIS_FORECAST_WAV_001_027. Issue 1.0. https://resources.marine.copernicus.eu/documents/PUM/CMEMS-GLO-PUM-001-027.pdf

CMEMS, 2018f – Product user manual for Regional High Resolution Sea Ice Charts Svalbard Region - SEAICE_ARC_SEAICE_L4_NRT_OBSERVATIONS_011_002. Issue 2.7. https://resources.marine.copernicus.eu/documents/PUM/CMEMS-SI-PUM-011-002.pdf

Coltman, N., Golding, N., Verling, E., 2008. Developing a broadscale predictive EUNIS habitat map for the MESH study area. 16 pp. Available online at http://www.searchmesh.net/pdf/MESH%20EUNIS%20model.pdf

JNCC, 2019. Prediction of outcrops or subcrops of rock in UK shelf seabed. https://doi.org/10.25603/840424.1.0.0 available at: https://data.gov.uk/dataset/fee92896-76a9-4718-a576-cd0d42224751/prediction-of-outcrops-or-subcrops-of-rock-in-uk-shelf-seabed-public

EMODnet Bathymetry Consortium, 2018. EMODnet Digital Bathymetry (DTM 2018). EMODnet Bathymetry Consortium. https://doi.org/10.12770/18ff0d48-b203-4a65-94a9-5fd8b0ec35f6

EMODnet Bathymetry Consortium, 2019 - High Resolution Seabed Mapping - WP2 : Generate indicators in the DTM - Use of the dataset Quality Index to expand services associated to the EMODnet DTM

Gorman, D., Bajjouk, T., Populus, J., Vasquez, M., Ehrhold, A., 2012. Modeling kelp forest distribution and biomass along temperate rocky coastlines. Marine Biology. https://doi.org/10.1007/s00227-012-2089-0

Hammar L., Schmidtbauer Crona, J., Kågesten, G., Hume, D., Pålsson, J., Aarsrud, M., Mattsson, D., Åberg, F., Hallberg, M., Johansson, T., 2018. Symphony, Integrerat planeringsstöd för statlig havsplanering utifrån en ekosystemansats. Havs- och vattenmyndighetens rapport

Kelly, N.M., Fonseca, M., Whitfield, P., 2001. Predictive mapping for management and conservation of seagrass beds in North Carolina. Aquat Conserv Mar Freshw Ecosyst

Lappalainen, J., Virtanen, E.A., Kallio, K., Junttila, S., Viitasalo, M., 2019. Substrate limitation of a habitat-forming genus Fucus under different water clarity scenarios in the northern Baltic Sea. Estuarine, Coastal and Shelf Science 218, 31–38. https://doi.org/10.1016/j.ecss.2018.11.010

Manca E., Lillis H., Annunziatellis A., Agnesi S., Mo G., Tunesi L., Parry M., Doncheva V., Al-Hamdani Z., 2017. The MSFD Benthic Broad Habitat Types Tables. Annex to : Populus et al, 2017. https://doi.org/10.13155/49975

Mariani, S., M. Casaioli, E. Coraci, and P. Malguzzi, 2015. A new high-resolution BOLAM-MOLOCH suite for the SIMM forecasting system: assessment over two HyMeX intense observation periods. Nat. Hazards Earth Syst. Sci., 15, 1–24, DOI:10.5194/nhess-15-1-2015

Mata Chacón, D., Sanz Alonso, J.L., Gonçalves, J.M.S., Monteiro, P., Bentes, L., McGrath, F., Henriques, V., Freitas, R., Amorim, P., Tempera, F., Fossecave, P., Alonso, C., Galparsoro, I., Vasquez, M., Populus, J., 2013. Report on collation of historic maps. Bathymetry, substrate and habitats - MeshAtlantic Report. Spanish Institute of Oceanography. 98 pp.

Populus, J., Vasquez, M., Albrecht, J., Manca, E., Agnesi, S., Al Hamdani, Z., Andersen, J., Annunziatellis, A., Bekkby, T., Bruschi, A., Doncheva, V., Drakopoulou, V., Duncan, G., Inghilesi, R., Kyriakidou, C., Lalli, F., Lillis, H., Mo, G., Muresan, M., Salomidi, M., Sakellariou, D., Simboura, M., Teaca, A., Tezcan, D., Todorova, V., Tunesi, L., 2017. EUSeaMap. A European broad-scale seabed habitat map. https://doi.org/10.13155/49975

Saulquin, B., Hamdi, A., Gohin, F., Populus, J., Mangin, A., d' Andon, O.F., 2013. Estimation of the diffuse attenuation coefficient KdPAR using MERIS and application to seabed habitat mapping. Remote Sensing of Environment 128, 224–233. doi: 10.1016/j.rse.2012.10.002.

Vasquez, M., Mata Chacon D., Tempera, F., O'Keeffe, E., Galparsoro, I., Sanz Alonso J. L., Goncalves Jorge M. S., Bentes, L., Amorim, P., Henriques, V., Mcgrath, F., Monteiro, P., Mende, B., Freitas, R., Martins, R., Populus, J., 2015. Broad-scale mapping of seafloor habitats in the north-east Atlantic using existing environmental data. Journal Of Sea Research, 100, 120-132. doi: 10.1016/j.seares.2014.09.011.

Virtanen, E.A., Viitasalo, M., Lappalainen, J., Moilanen, A., 2018. Evaluation, Gap Analysis, and Potential Expansion of the Finnish Marine Protected Area Network. Front. Mar. Sci. 5. https://doi.org/10.3389/fmars.2018.00402

Virtanen, E., Niemelä, W., Bekkby, T., Gonçalves, J., Laamanen, L., Lillis, H., Manca, E., Pesch, R., Tempera, F., Vasquez, M., Viitasalo, M., Castle, L., O'Keeffe, E., 2019. Review and compilation of habitat models in European Seas, Report

8 Annex 1 - Compiling oceanographic layers

Roberto Inghilesi, National Centre for Environmental Crisis, Emergencies and Damage – Operational Centre for Environmental Monitoring – ISPRA

Roberto.inghilesi@isprambiente.it

8.1 Introduction

The aim of the work for the period 2017-2019 was to complete the oceanographic data coverage and improve the quality of some products already provided in the previous phases. Given the upgrades made in 2016 in some of the Copernicus Marine Environment Monitoring System (CMEMS) model implementations, high resolution sea-bottom energy products have been recalculated for the Mediterranean Sea (currents), Black Sea (currents), Iberian-Biscay-Ireland and Macaronesia (currents and waves). The wave energy products have also been evaluated at 1m depth from the bottom using a simplified boundary layer post-processing. A special nested implementation of Wave Model has been set up by ISPRA in the Black Sea in order to reach approximately 3x3km resolution, using high quality wind at 7.5 km resolution and the EMODNET Bathymetry 2016. Potential density at the sea bottom has been evaluated based on salinity and potential temperature fields provided by CMEMS. All products have been statistically analyzed to provide the relevant statistical operator (90th percentile or average in the case of salinity). In the following sections of the report, the methods used to evaluate the energy at the sea bottom for currents are presented in section 2, the estimate of the potential density in the Black Sea is presented in section 3 and the method used to evaluate the energy at the sea bottom for waves is presented in section 4. The results, mapped in each areas of interest, are also illustrated.

8.2 Estimate of the energy density due to currents at the sea bottom

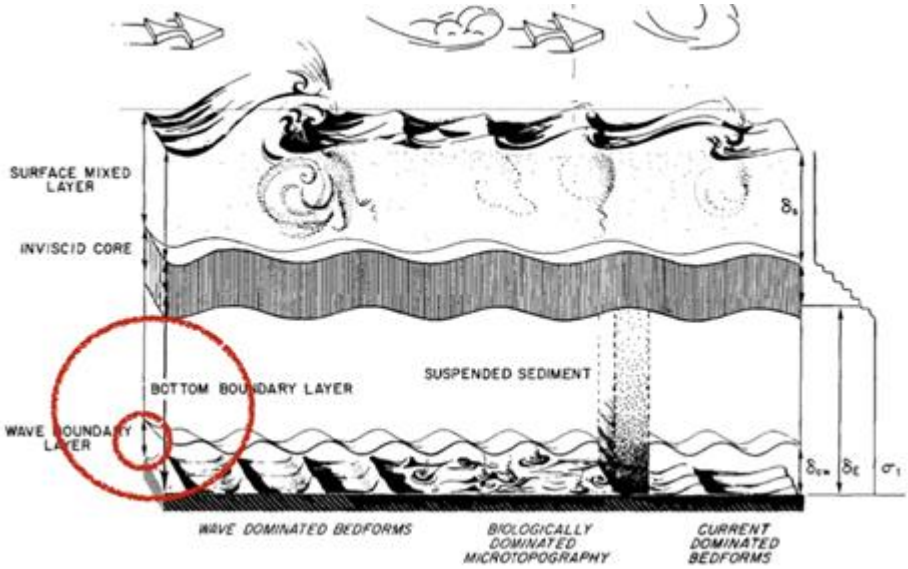

The European Marine Observation and Data Network (EMODnet) is financed by the European Union under Regulation (EU) No 508/2014 of the European Parliament and of the Council of 15 May 2014 on the European Maritime and Fisheries Fund.

Figure 8.1: schematic view of the oceanic processes, evidenced in red are the bottom boundary layer due to waves and currents (Grant et al. 1986)

In the lowest part of the ocean, where the drag due to the presence of the sea bottom strongly modifies the water currents (Figure 1) there are characteristic regions where the relationship between the vertical variation of the current and the distance from the bottom can be established (Figure 2).

In the overlap layer, which is relatively close to the bottom, the current follows the well-known logarithmic law of the wall, i.e.

$$u(z) = \frac{u_*}{\kappa}\log(\frac{z}{z_0}) \qquad (1)$$

where u(z) is the current at the depth z, u_* is the friction velocity, k is the constant of Von Karman, z_0 is the roughness length. The expression holds sufficiently close (but not too much) to the bottom, say for

$$z < 0.4\frac{u_*}{f} \qquad (2)$$

where f is the Coriolis parameter, which depends on the latitude and the velocity of the Earth.

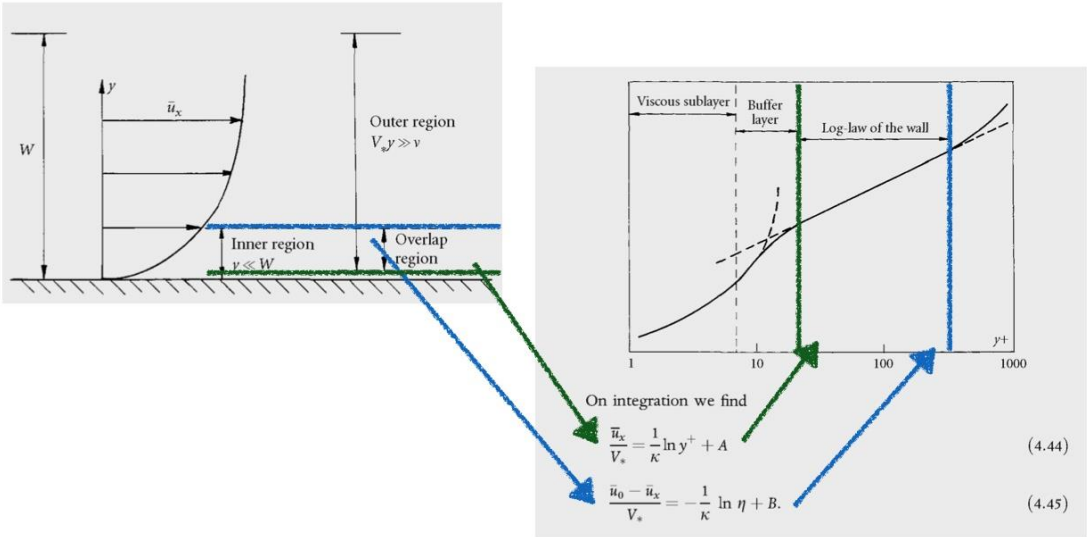

Figure 8.2: Schematic view of the overlap region and the log-law of the wall (Davidson, 2004)

Assuming that the bottom roughness does not vary too much, neutral stratification, and taking for z_0 a constant averaged value, the essential problem is to evaluate the u_* or, in other words, the model of turbulence. Since the data currents in CMEMS archive are calculated using the oceanic model NEMO, the same turbulence parameterization of the model has been used for the post processing of the data. In NEMO the effect of the bottom friction is obtained using a quadratic bottom drag with logarithmic formulation,

$$u_*^2 = C_D u^2 \qquad (3)$$, and

$$C_D = \max\{C_{Dmin}, \frac{1}{\kappa}\log(\frac{dz_B}{2z_0})^{-2}\} \qquad (4)$$

where u is the current in a layer above the overlap layer, C_D is the drag factor, C_{Dmin} is a constant value, dz_B is the thickness of the model layer closest to the bottom. (Maraldi et al., 2013)

The numerical algorithm works in the following way:

1. At each point of the grid, from the vertical profile of the current given by the oceanographic model (Figure 3), find the first level above the bottom. Evaluate the distance from the sea bottom using the EMODNET bathymetry. Evaluate the thickness of the last layer of the model (Figure 4).
2. Evaluate the friction velocity from (3) using (4). Verify that the depth of the layer is not too shallow using (2). If the reference level is too close to the ground, then repeat 1. and 2. at the next model level.
3. Evaluate the current at z=1m using (1), and then the energy at the seabottom $E_{SB} = \frac{1}{2}\rho u^2$.
4. The energy layers in all the 2016-2018 period of time have been processed in order to determine the 90th percentile.

The numerical constant used in the calculations are:

C_{Dmin}=0.0025, z_0=0.0035m, $\kappa = 0.4$, $\rho = 1036$ kg/m^3

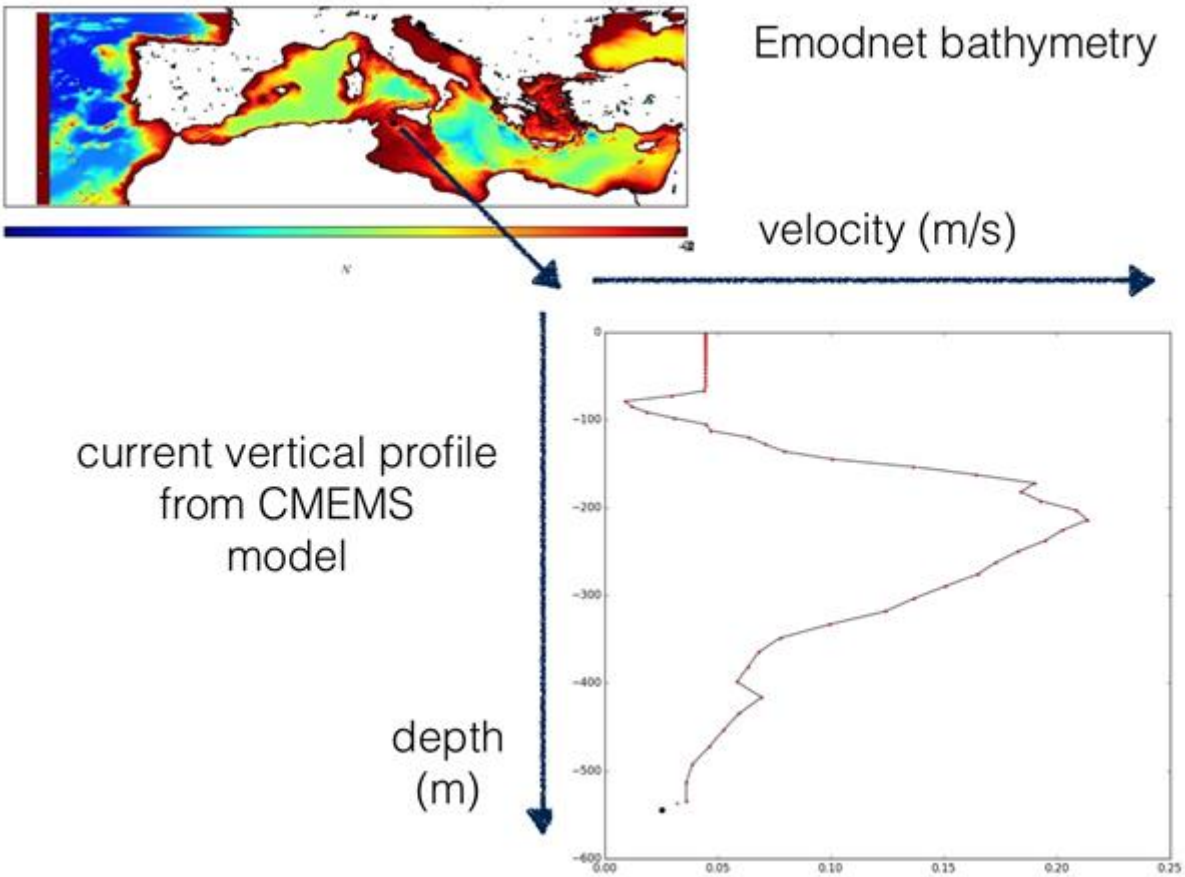

Figure 8.3: vertical profile of velocity in a point of the central Mediterranean Sea. Black dot at the end of the profile is the estimate of the current at 1m from the sea bottom

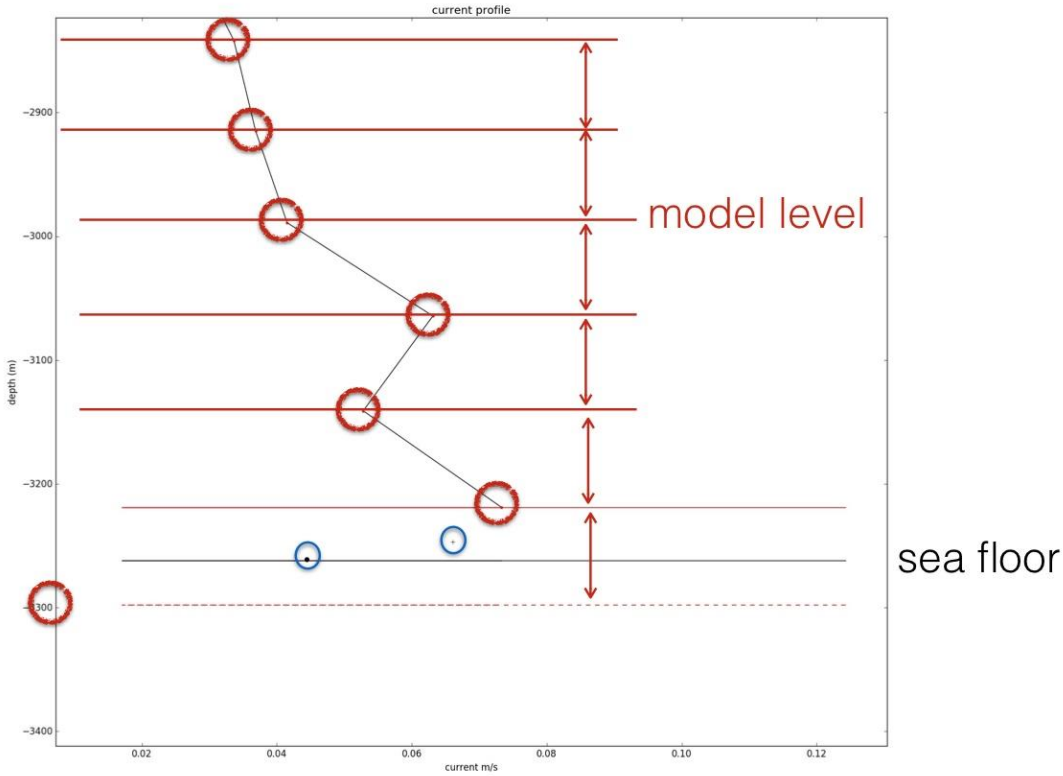

Figure 8.4: bottom part of the vertical profile of velocity in a point of the Mediterranean Sea. Black dot at the end of the profile is the estimate of the current at 1m from the sea bottom. Evidenced in red are the oceanographic model levels.

The post processing has been applied to:

1. the Mediterranean Sea using the CMEMS product MEDSEA_ANALYSIS_FORECAST_PHY_006_013 with resolution 0.042x0.042 deg. and 141 vertical levels (Figure 5);
2. the Iberian-Biscay-Irish area using the CMEMS product ATLANTIC-IBI_ANALYSIS_FORECAST_PHY_005_001 with resolution 0.028x0.028 deg. and 50 vertical levels (Figure 6);
3. the Macaronesia area using the CMEMS product ATLANTIC-IBI_ANALYSIS_FORECAST_PHY_005_001 with resolution 0.028x0.028 deg. and 50 vertical levels (Figure 7);
4. the Black Sea using the CMEMS product BLKSEA_ANALYSIS_FORECAST_PHYS_007_001 with resolution 0.028x0.037 deg. and 31 vertical levels (Figure 8);

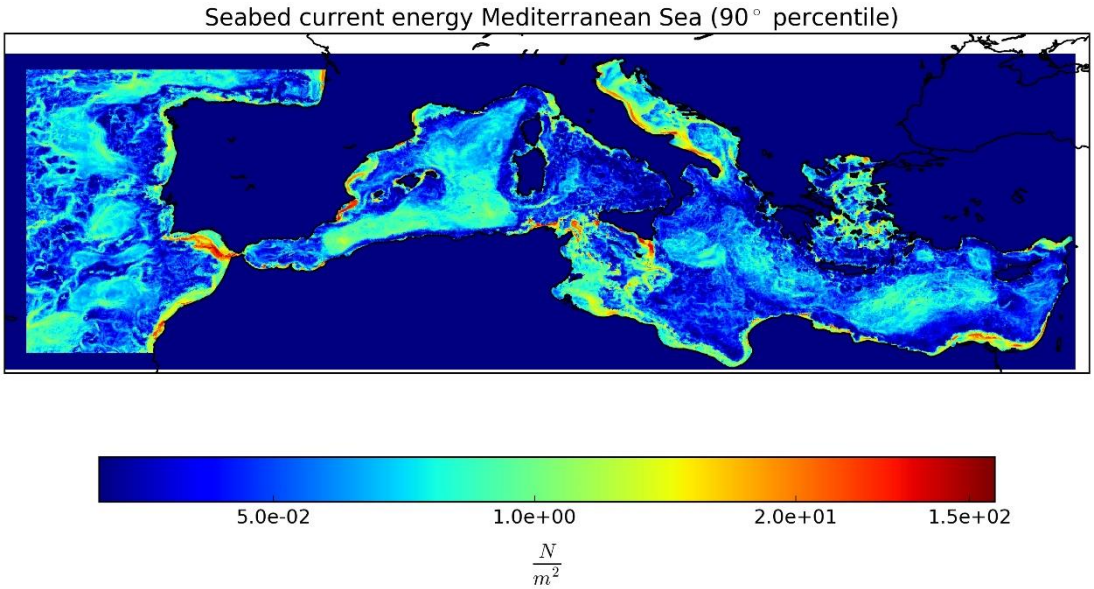

Figure 8.5: Energy at the seabed (1m) due to currents in the Mediterranean Sea (90th percentile 2016-2018)

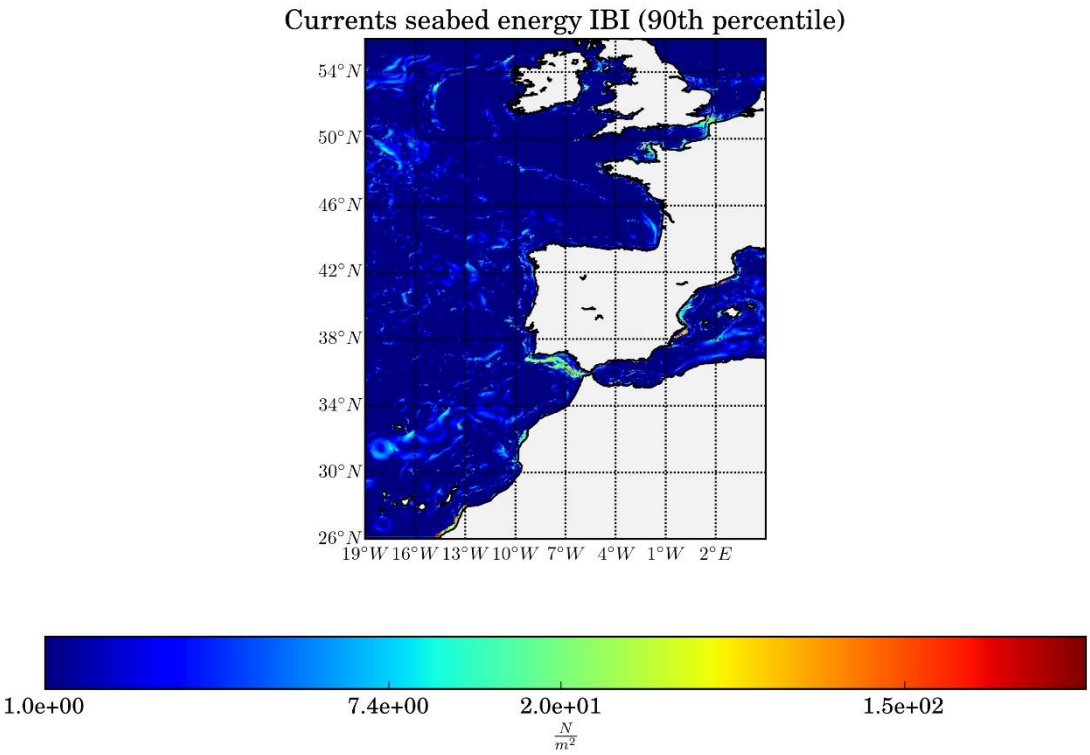

Figure 8.6: Energy at the seabed (1m) due to currents in the Iberian-Biscay- Irish Ocean (90th percentile 2012-2018)

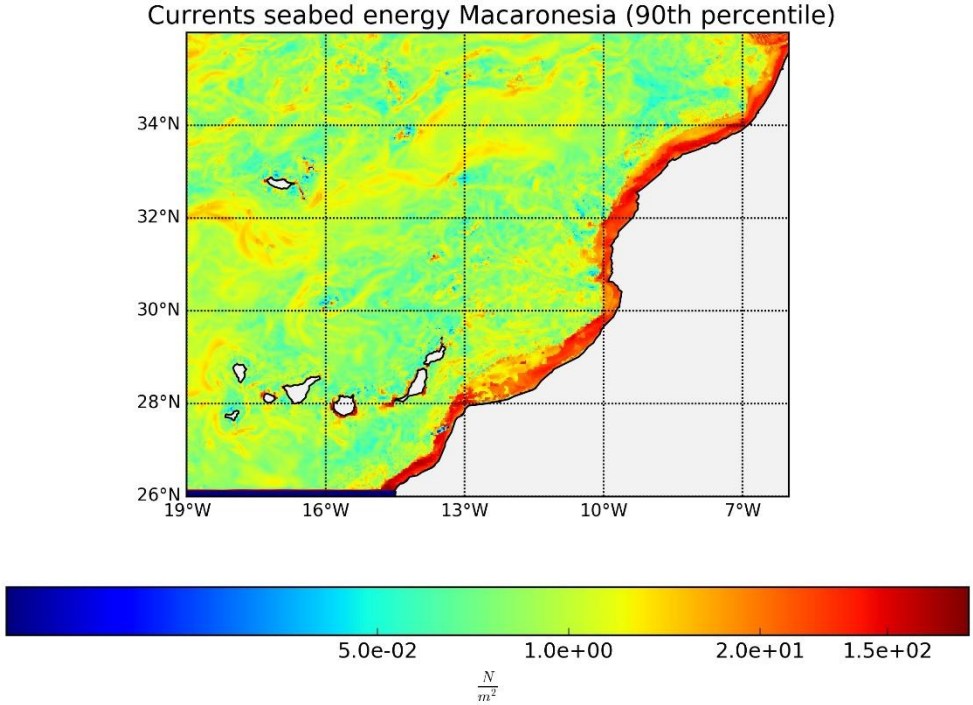

Figure 8.7: Energy at the seabed (1m) due to currents in the Macaronesia (90th percentile 2016-2018)

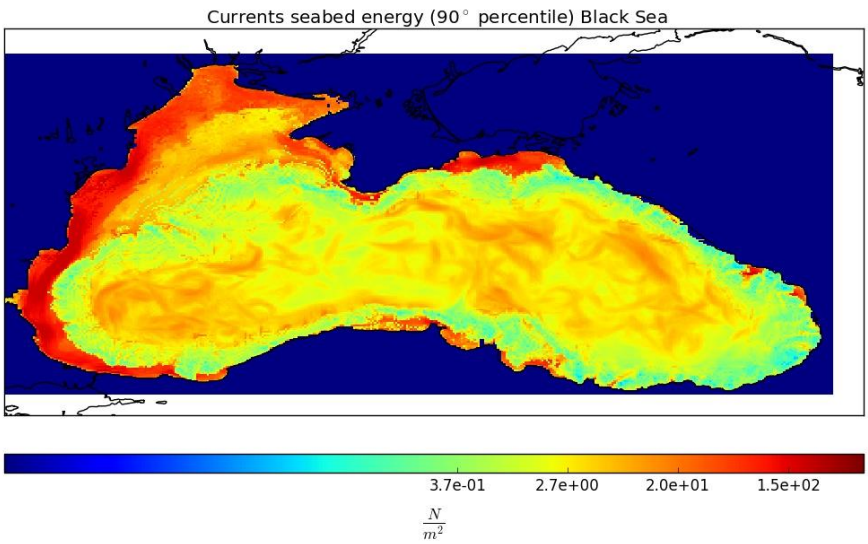

Figure 8.8: Energy at the seabed (1m) due to currents in the Black Sea (90th percentile 2016-2018)

8.3 Evaluation of the potential density at the sea bottom in the Black Sea

The potential density at the bottom of the Black Sea has been evaluated from the temperature at the bottom provided by CMEMS, the 3D field of salinity SU04-BS-CMCC-SAL-REAN-M provided by CMEMS and the bathymetry provided by EMODNET Bathymetry.

Since the salinity varies almost monotonically close to the bottom, (Figure 9), the post processing is easier than for the currents.

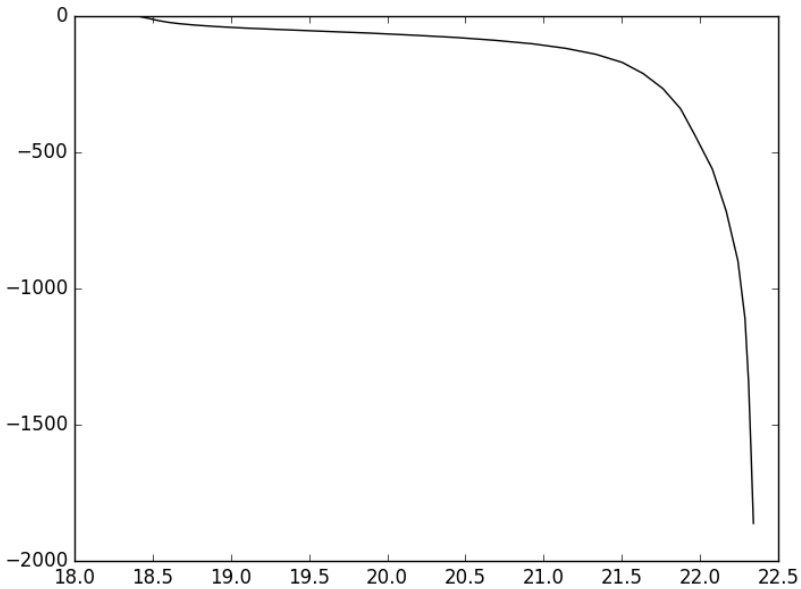

Figure 8.9: Example of vertical profile of salinity in the Black Sea from oceanographic model

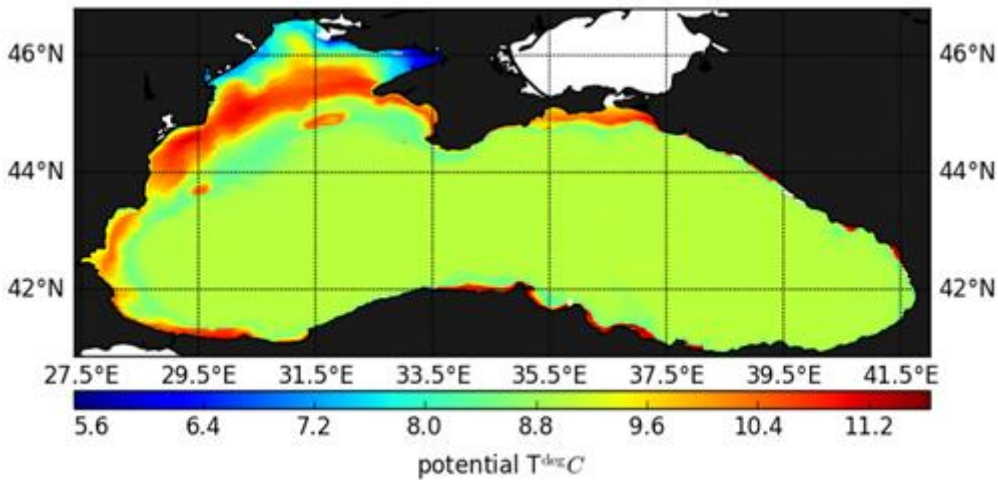

Figure 8.10: Potential temperature at the sea bottom in the Black Sea

Algorithm:

First step: determine the salinity in the layer close to the sea bottom using the vertical profiles of salinity (Figure 11);

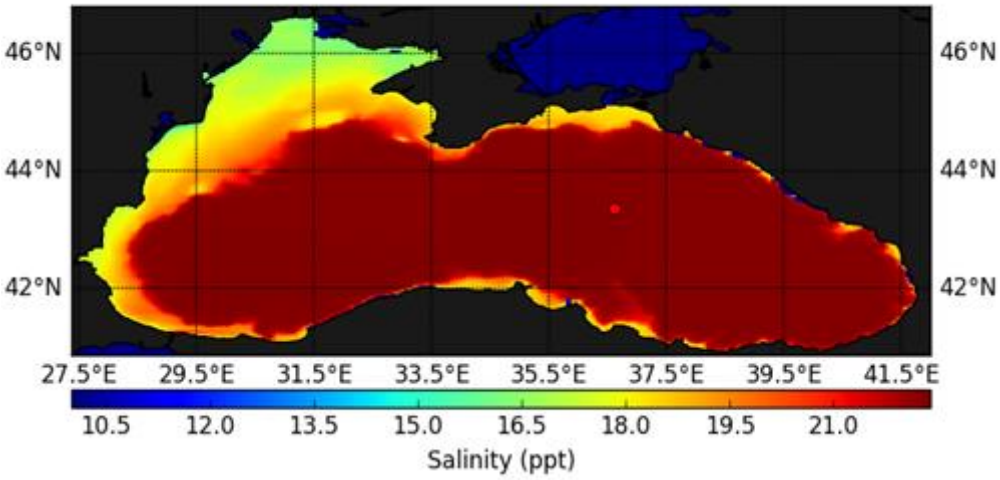

Figure 8.11: Salinity at the sea bottom in the Black Sea

Second step: using the potential temperature at the bottom (Figure 10) and the salinity at the bottom in the UNESCO 1981 formula, determine the σ_ϑ (Figure 12)

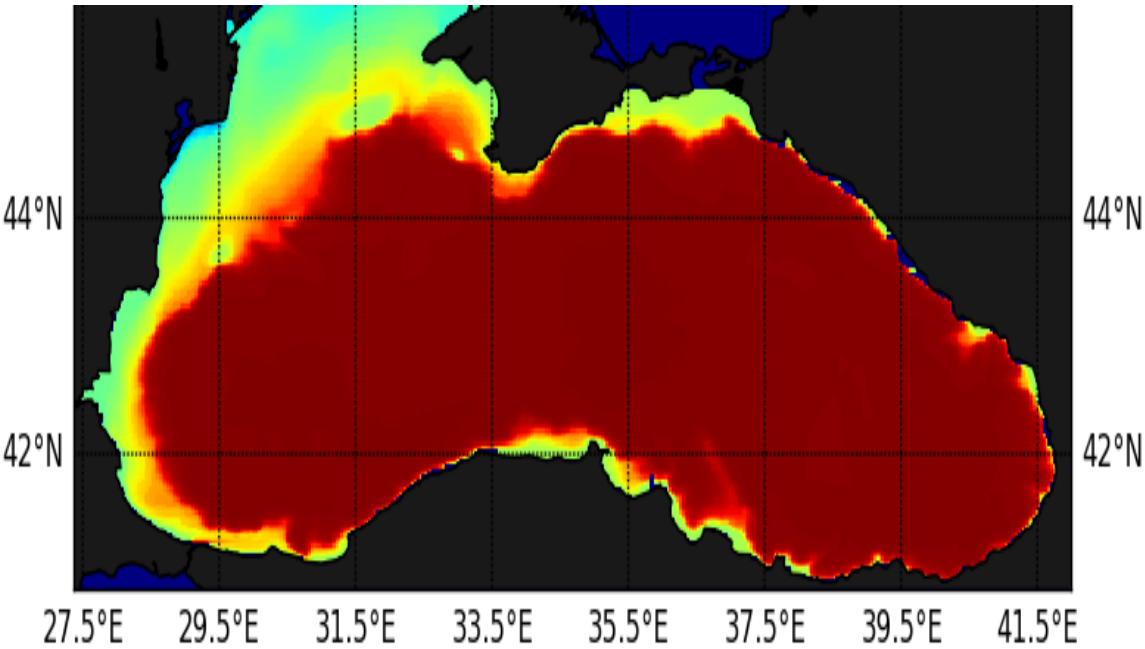

Figure 8.12: Potential density at the sea bottom in the Black Sea

Third step: evaluate the potential density for all the available periods to evaluate the average value (Figure 13).

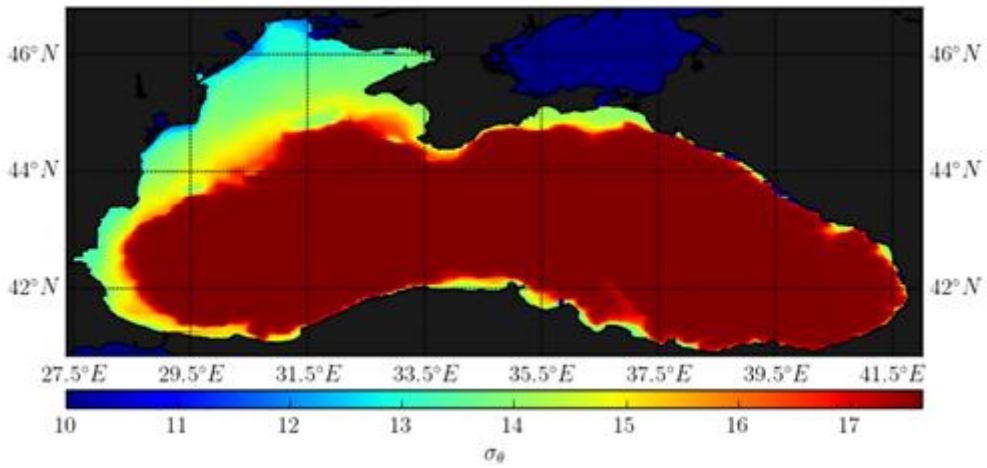

Figure 8.13: Average potential density at the sea bottom in the Black Sea 2011-2018

8.4 Estimate of the 90th percentile of sea-bottom kinetic energy

The peak kinetic energy (KE) at the bottom has been calculated in the Black Sea using wave data series provided by ISPRA using a special implementation of the Wave Model. The set-up configuration was based on a large scale run on a grid at 1/64 deg. on the whole Black Sea. Two very high-resolution grids (West and East Black Sea) at 1/128 deg. resolution were nested on the large-scale run. A 7.5km resolution BOLAM wind was used in the period 2016-2018 to provide the meteorological forcing, while the numerical bathymetry was based on the EMODNET bathymetry DTM product realised in 2016. The runs were executed on a HPC cluster of 16 nodes at ISPRA. In the Macaronesia area the sea bottom energy was estimated using the CMEMS product of global analysis GLOBAL_ANALYSIS_FORECAST_WAV_001_027 at resolution 1/12 deg.

The spatial distribution of the percentile 90th of the kinetic energy at the bottom has been estimated by considering the statistics in the time period available at each grid point. In order to evaluate the KE at the bottom due to a single monochromatic wave, the first step could be to estimate the orbital velocity at the bottom (Ub), then the energy would be given by $E_b = \frac{1}{2}\rho U_b^2$, given ρ the average density of seawater. In literature there are several straightforward algorithms based on the linear theory of wave propagation which could be easily used to estimate the orbital velocity under the waves as $\mathrm{U_b} = \frac{\mathrm{H}}{2}\frac{\omega}{\sinh(\mathrm{kh})}$.

The methods are easily implemented for monochromatic waves in terms of the angular frequency of the wave (ω), the wave height (H), the wavelength (k) of the wave and the local depth of the sea (k). The frequency and the wavelength are related by the dispersion formula $\omega^2 = \mathrm{gktanh(kh)}$

In the real sea, though, the significant wave height (H_{m0}) is a statistical parameter associated with the effect of the superposition of a large number of waves, each one at a different frequency. A Method for evaluating the energy associated with realistic situations, using reasonably assumptions about the spectral form of the waves, is described in Soulsby (1987).

Here a simplified version of the method, the 'Soulsby and Smallman' method, has been applied (Soulsby, 2006). The method prescribes the use of an approximation formula, which provides the variance of the velocity $\mathrm{U_{rms}^2}$ at the bottom with an accuracy better than 1% where the velocities are significantly different from zero.

$$\frac{U_{rms}T_n}{H_{m0}} = \frac{0.25}{(1 + At^2)^3}$$

$$A = (6500 + (0.56 + 15.54t)^6)^{\frac{1}{6}}$$

$$t = \frac{T_n}{T_m}$$

$$T_n = \left(\frac{h}{g}\right)^{\frac{1}{2}}$$

Where h is the depth of the bottom sea and g is the gravity acceleration. The inputs to the algorithm are the H_{m0}, T_m, and *h* on the WAM grids. The bottom KE due to the field of random waves is then evaluated as $\mathrm{E_b} = \frac{1}{2}\rho \mathrm{U_{rms}^2}$.

To obtain the spatial distribution of the 90-percentile of seabed energy due to wind waves, the hourly bottom energy fields have been statistically analysed in the period 2016 –2018.

The post processing has been applied to:

1. the Black Sea using the ISPRA high resolution WAM at resolution 1/64, the BOLAM wind at resolution 7.5km, and EMODNET bathymetry (Figure 14);
2. the western Black Sea using the very high resolution ISPRA WAM at resolution 1/128, the BOLAM wind at resolution 7.5km, and EMODNET bathymetry (Figure 15);
3. the eastern Black Sea using the very high resolution ISPRA WAM at resolution 1/128, the BOLAM wind at resolution 7.5km, and EMODNET bathymetry (Figure 16);
4. the Macaronesia using the low resolution CMEMS product of global analysis GLOBAL_ANALYSIS_FORECAST_WAV_001_027 at resolution 0.083x0.083 and EMODNET bathymetry (Figure 17).

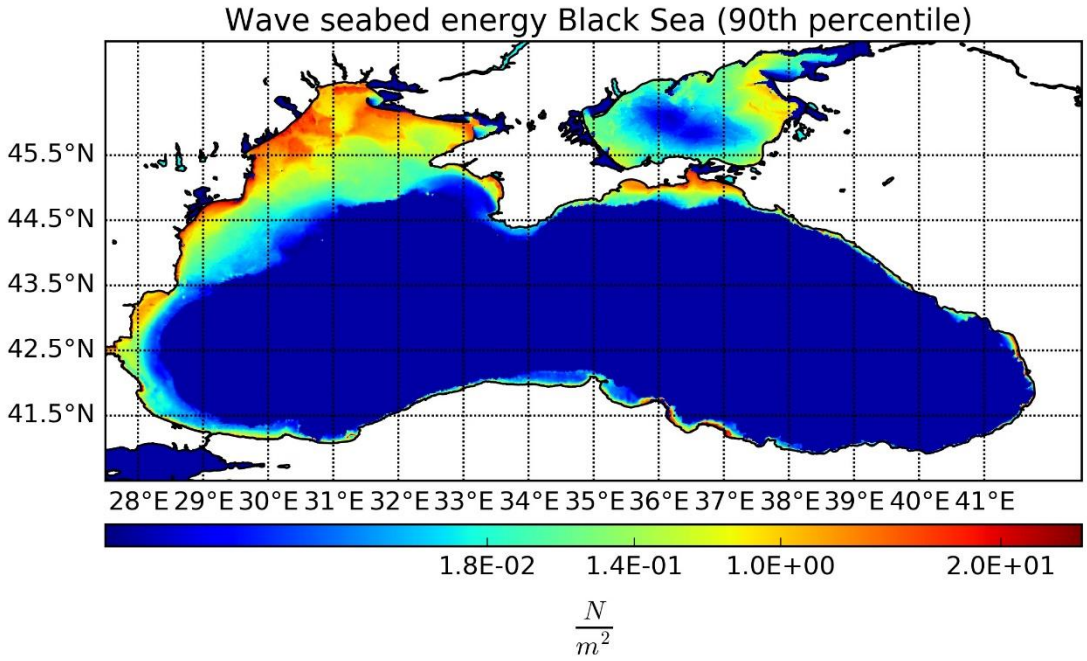

Figure 8.14: Energy at the seabed (1m) due to wind waves in the Black Sea (90th percentile 2016-2018)

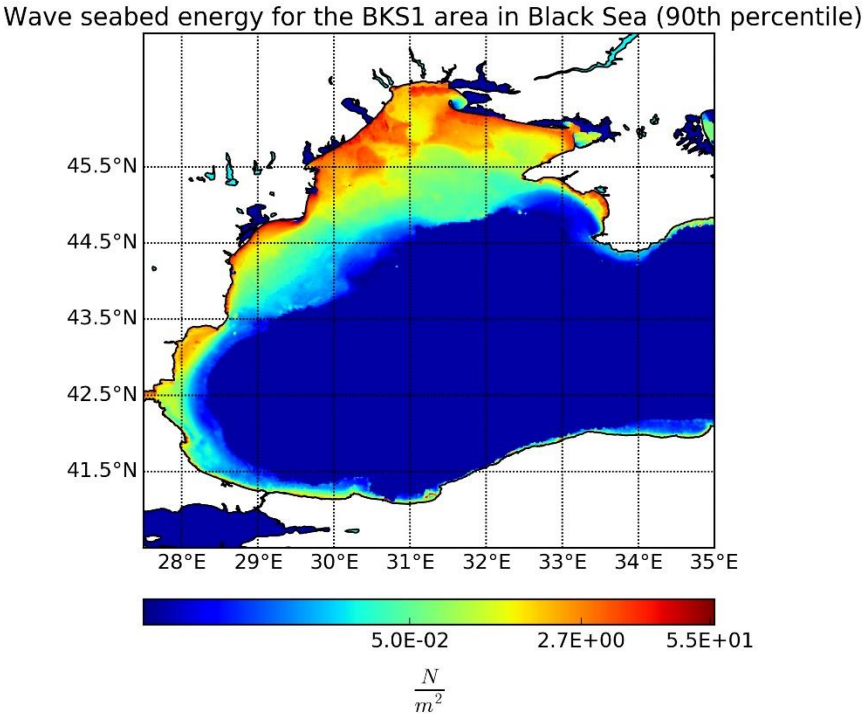

Figure 8.15: Energy at the seabed (1m) due to wind waves in the western Black Sea (90th percentile 2016-2018)

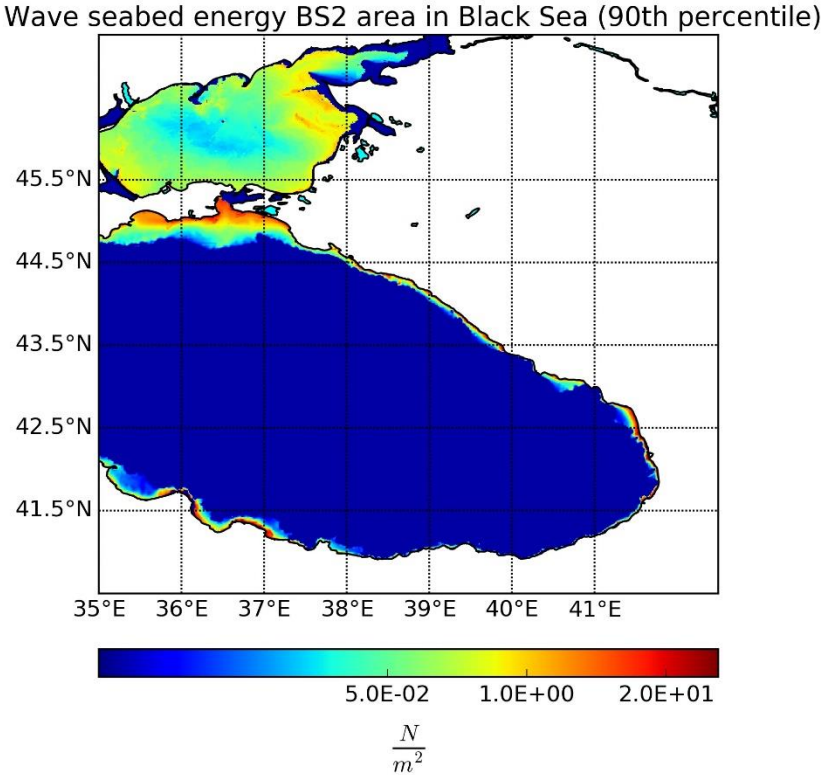

Figure 8.16: Energy at the seabed (1m) due to wind waves in the eastern Black Sea (90th percentile 2016-2018)

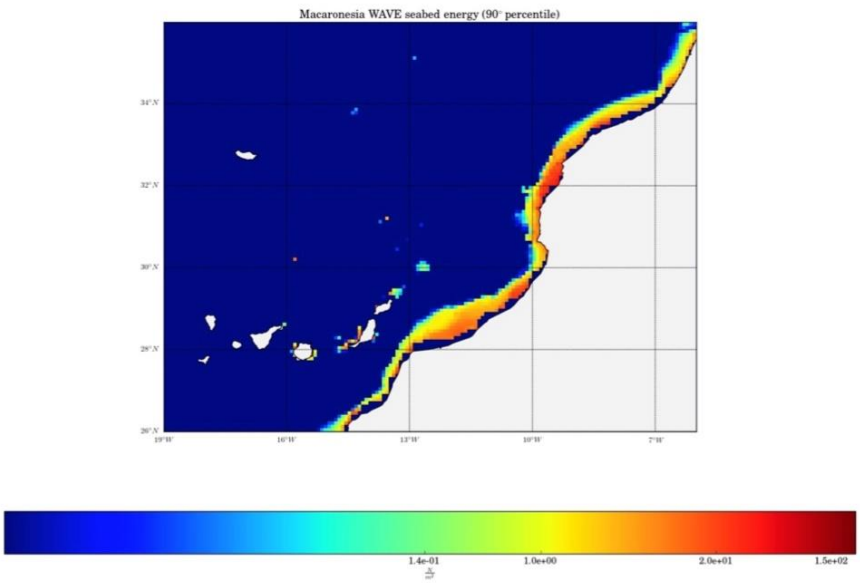

Figure 8.17: Energy at the seabed (1m) due to wind waves in Macaronesia (90th percentile 2016-2018)

8.5 References

Casaioli M., Catini F., Inghilesi R., Lanucara P., Malguzzi P., Mariani S, and Orasi A., 2014. An operational forecasting system for the meteorological and marine conditions in Mediterranean regional and coastal areas. Adv. Sci. Res., 11, 11–23.

P.A. Davidson, 2004, Turbulence, An introduction for scientists and engineers, Oxford University Press.

P. Fofonoff, R.C. Millard Jr., 1983, Algorithms for computation of fundamental properties of seawater, UNESCO technical papers in marine science n.44.

W.D. Grant, O.S. Marsden, 1986, The Continental Shelf Bottom Boundary Layer, Ann. Rev. Fluid Mech. 18,265-305

Inghilesi R., Catini F., Franco L. , Bellotti G., Orasi A. and Corsini S., 2012. Implementation and test of a coastal forecasting system for wind waves in the Mediterranean Sea. Nat. Hazards Earth Syst. Sci., 12, 485-494.

Janssen, P.A.E.M. (2004),The interaction of ocean waves and wind, Cambridge University Press

Janssen P.A.E.M., 2008. Progress in ocean wave forecasting, Journal of Computational Physics Volume 227, Issue 7, 20 March 2008, Pages 3572–3594

Komen, G.J., L. Cavaleri, M. Donelan, K. Hasselmann, S. Hasselmann, and P.A.E.M. Janssen, 1994. Dynamics and Modelling of Ocean Waves. Cambridge University Press, Cambridge.

C. Maraldi, J. Chanut, B. Levier, N. Ayoub, P. De Mey, G. Reffray, F. Lyard, S. Cailleau, M. Drévillon, E. A. Fanjul, M. G. Sotillo, P. Marsaleix, and the Mercator Research and Development Team, 2013, NEMO on the shelf: assessment of the Iberia–Biscay–Ireland configuration, Ocean Sci., 9, 745-771, 2013

A. Perlin, J. N. Moum, J. M. Klymak, M. D. Levine, T. Boyd, and P. M. Kosro, 2005, A modified law-of-the-wall applied to oceanic bottom boundary layers Journal Geophys. Res. Vol.106, C3, 4421-4435.

Soulsby R., 1997. Dynamics of marine sands. A manual of practical applications. Thomas Telford Publications. 249 pp.

Soulsby R.L., 1987. Calculating Bottom Orbital Velocity Beneath Waves, Coastal Engeenering 11 (1987), 371-380.

Soulsby R.L. and Clarke S., 2005. Bed shear-stresses under combined waves and currents on smooth and rough beds Produced within Defra project FD1905 (EstProc). Report TR 137 - Rev 1.0 - August 2005 - HR Wallingford.

Soulsby R.L., 2006. Simplified calculation of wave orbital velocities, report TR 155, HR Wallingfort

A. Soloviev, R. Luckas, P.Hacker, 2001, An approach to parameterization of the oceanic turbulent boundary layer in the western Pacific warm pool, Journal Geophys. Res. Vol.106, C3, 4421-4435.

G.L. Weatherly, P.J. Martin, 1978, On the Structure and Dynamics of the Oceanic Bottom Boundary Layer, J. Phys. Ocean. 8, 557-570

9 Annex 2 – EUSeaMap in EUNIS 2007-2011

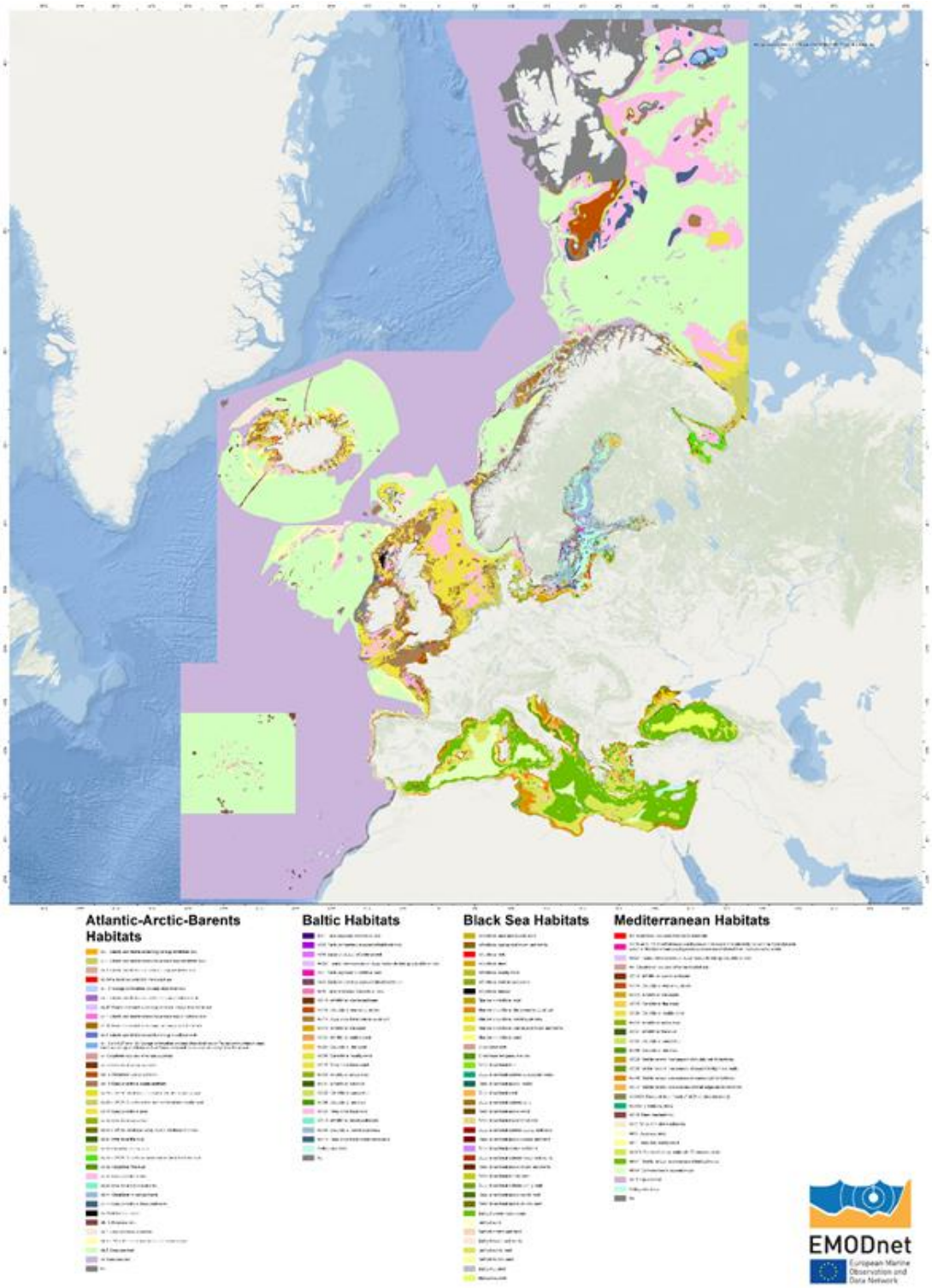

The European Marine Observation and Data Network (EMODnet) is financed by the European Union under Regulation (EU) No 508/2014 of the European Parliament and of the Council of 15 May 2014 on the European Maritime and Fisheries Fund.

10 Annex 3 – Habitat classification updates in the Black Sea

Mickaël Vasquez – Ifremer
Mickael.Vasquez@ifremer.fr
Valentina Todorova - IO-BAS
vtodorova@io-bas.bg
Valentina Doncheva - IO-BAS
valentina.doncheva@gmail.com
Mihaela Muresan - GeoEcoMar
mmuresan@geoecomar.ro
Adrian Teaca - GeoEcoMar
adrianxteaca@yahoo.com

A workshop on the assessment of EUSeaMap 2016 in the Black Sea was held in Varna on April 11th-12th, 2018. Some shortcomings were identified which led to a major update to the broad-scale habitat classification that was developed during phase 2 of EMODnet Seabed Habitats.

One major decision was to follow the recommendations of Berov et al (2018) and assign the algal association red and brown macroalgae *Phyllophora crispa, Zanardinia typus, Apoglossum ruscifolium*) and/or widely adaptive green algae *Cladophora albida, Cladophora coelothrix* and red macroalgae *Polysiphonia elongata, Gelidium spinosum, Gelidium crinale)*, although named "sciaphilic", to the infralittoral zone, due to the light conditions normally associated with that zone as well as the dominance of erect perennial macroalgae, especially *Phyllophora crispa*. Berov et al (2018) also argue that in the circalittoral the only prominent macroalgal species is the red alga *Antithamnion cruciatum*.

It was also discussed that shell-dominated sediments found on the Romanian coast, and which are acknowledged to have quite an extensive spatial distribution, were not captured in the seabed substrate map provided by EMODnet Geology. A sediment matrix mixed with a substantial amount of shelly debris should be classified as "mixed sediment". However, in the EMODnet Geology map, these sediments on the Romanian coast are systematically classified as "mud". In phase 2 this shortcoming drove to clamp together several habitats, e.g. "shallow circalittoral mud" and "shallow circalittoral organogenic sandy mud/muddy sand". These two habitats host quite different communities (the former contains "Muds with Abra nitida, Pitar rudis, Spisula subtruncata, Acanthocardia paucicostata and Nephtys hombergii" and the latter hosts "Muddy sand with Dipolydora quadrilobata meadows and Mytilus galloprovincialis"). Classifying shell-dominated sediments into either of these classes constitutes a substantial loss of information which could have serious management implications. Based on the knowledge of the participants the area of shelly substrate was reclassified as "mixed sediment" replacing the areas classed as "mud" in the EMODnet Geology layer.

10.1 Broad-scale habitat classification

The general rules used to model regional sea habitats in EUSeaMap are inadequate in areas that have a high concentration of freshwater fine sediments. These areas were called plume areas and were delimited using expert knowledge. In the Black Sea, two plume areas (Figure 10.1), influenced by the Dnieper-Bug and Danube rivers, were defined as part of EMODnet phase 2 (Populus et al, 2017).

The European Marine Observation and Data Network (EMODnet) is financed by the European Union under Regulation (EU) No 508/2014 of the European Parliament and of the Council of 15 May 2014 on the European Maritime and Fisheries Fund.

Figure 10.1: Spatial distribution of plume areas (dark grey)

The tables below describe the habitats that occur inside and outside of the plume areas.

Columns: Bioz. = Biological zone; Susb. = substrate; Ox. = Oxygen conditions

Biological zones: infra. = infralittoral; circa. = circalittoral; abys. = abyssal

Oxygen conditions: subox. = suboxic; anox. = anoxic

Table 10.1*: H*abitats occurring inside the plume areas

Habitat	Bioz.	Subs.	Ox.	Communities
Infralittoral sand	infra.	sand		Fine sand with *Lentidium mediterraneum*
Infralittoral muddy sand	infra.	muddy sand		*Cerastoderma glaucum, Mya arenaria, Anadara kagoshimensis*
Circalittoral coarse and mixed sediment	circa.	mixed coarse		Diverse faunal assamblages due to hetergenous substrate dominated by bivalves *Mytilus galloprovincialis, Spisula subtruncata, Acanthocardia paucicostata* and polichaetes *Nephtys hombergii*
Circalittoral terrigenous muds	circa.	mud sandy mud		Danube and Dnieper plume areas (Mud with *Melinna palmata, Mya arenaria, Alitta succinea, Nephtys hombergii)*

Table 10.2*:* Habitats occurring outside the plume areas

Habitat	Bioz.	Subs.	Ox.	Communities
Infralittoral rock	infra.	rock	oxic	*Upper-infralittoral rock dominated by Cystoseira bosphorica* *Upper-infralittoral rock dominated by Cystoseira barbata* *Upper infralittoral rock with variable annual green and red macroalgae Ceramium virgatum, Gelidium spinosum, G. crinale, Corallina mediterranea, Ulva rigida, Ulva linza, U. intestinalis, Cladophora sericea, C. albida, Bryopsis plumosa* *Lower infralittoral rock with dominant perennial sciaphylic red and brown macroalgae (Phyllophora crispa, Zanardinia typus, Apoglossum ruscifolium) and/or widely adaptive green (Cladophora albida, Cladophora coelothrix) and red macroalgae (Polysiphonia elongata, Gelidium spinosum, Gelidium crinale, Anithamniom cruciatum)* *Infralittoral rock overgown by Mytilaster lineatus and Mytilus galloprovincialis* *Infralittoral soft rock with piddocks (Pholas dactylus, Barnea candida)* *Infralittoral rock with faunal turf (bryozoans, sponges)* *Biogenic reefs of Ostrea edulis* *Upper infralittoral rock with photophilic macroalgae (Ceramium virgatum, Corallina officinalis, Ulva rigida, Ulva linza, U. intestinalis, Cladophora vagabunda, Cladophora sericea, C. albida, Bryopsis plumosa and Cystoseira barbata)* *Infralittoral rock with Mytilaster lineatus and Mytilus galloprovincialis* *Infralittoral soft rock with Pholadidae* *Lower infralittoral rock with faunal turf (sponges)*
Circalittoral rock	circa.	rock	oxic	Mussel beds of Mytilus galloprovincialis on varied circalittoral sediment Circalittoral rock overgrown by Mytilus galloprovincialis, hydrozoans and sponges
Infralittoral Coarse and Mixed Sediment	infra.	coarse mixed	oxic	Infralittoral shelly gravel and sand with *Chamelea gallina* and *Mytilus galloprovincialis*
Infralittoral sand and muddy sand	infra.	sand	oxic	Pontic Zostera noltii meadows Pontic mixed Zostera noltii- Zannichellia palustris-Zostera marina meadows

Habitat	Bioz.	Subs.	Ox.	Communities
		muddy sand		Pontic Zostera marina meadows Pontic Potamogeton petcinatus - Zannichellia palustris meadows in man-made sheltered areas Upper-infralittoral medium and fine sand dominated by Donax trunculus Infralittoral shelly coarse sand and shellbed with varied infauna Infralittoral fine and medium sand, dominated by Chamelea gallina (Lentidium mediterraneum, Tellina tenuis) Lower infralittoral coarse and medium sand, dominated by Upogebia pusilla Infralittoral fine sand dominated by Lentidium mediterraneum (Cerastoderma glaucum) Lower infralittoral muddy sand with Upogebia pusilla
Shallow circalittoral shelly coarse sediment	circa.	coarse	oxic	*Coccotylus truncatus & Phyllophora crispaon shelly organogenic sand* *Shallow circalittoral shelly coarse sediment with varied infauna (Modiolus adriaticus, Gouldia minima)* *Shallow circalittoral shelly coarse sediment with varied infauna (Nereididae, Diogenes pugilator, Polititapes aureus, Pitar rudis, Mytilus beds)*
Shallow circalittoral mud	circa.	mud sandy mud muddy sand	oxic	Shallow circalittoral muddy sand and sandy mud with Upogebia pusilla, Heteromastus filiformis, Nephtys hombergii, Aricidea claudiae, Chamelea gallina Shallow circalittoral mud dominated by Melinna palmata Shallow circalittoral sandy mud and mud with Pitar rudis, Spisula subtruncata, Paphia aurea, Mytilus galloprovincialis, Abra spp., Cardiidae, Nephthys hombergii, Heteromastus filiformis Shallow circalittoral mud and sandy mud with Upogebia pusilla (up to 30m depth) Shallow circalittoral mud with Abra nitida, Pitar rudis, Spisula subtruncata, Acanthocardia paucicostata, Nephthys hombergii and Mytilus galloprovinciali
Shallow circalittoral mixed sediment	circa.	mixed	oxic	Shallow circalittoral with Dipolydora quadrilobata meadows and Mytilus
Deep circalittoral muddy sand	deep circa.	muddy sand	oxic	Deep circalittoral muddy sand with tunicates

Habitat	Bioz.	Subs.	Ox.	Communities
Deep circalittoral mixed sediments	deep circa.	mixed	oxic	Deep circalittoral shelly mud with *Modiolula phaseolina*
Deep circalittoral mud	deep circa.	mud sandy mud	oxic	Deep circalittoral mud with *Terebellides stroemi*, *Amphiura stepanovi*, *Pachycerianthus solitarius*
Deep circalittoral suboxic calcareous muds	deep circa.	mud	subox.	Deep circalittoral suboxic muds with *Bougainvillia muscus*
Deep circalittoral anoxic muds	deep circa.	mud	anox.	
Bathyal anoxic muds	deep circa.	mud	anox.	
Abyssal seabed	abys.	any	anox.	

10.2 References

Berov D., Todorova T., Dimitrov L., Karamfilov V., 2018. Distribution and abundance of phytobenthic communities: Implications for connectivity and ecosystem functioning in a Black Sea Marine Protected Area Estuarine, Coastal and Shelf Science.

Populus, J., Vasquez, M., Albrecht, J., Manca, E., Agnesi, S., Al Hamdani, Z., Andersen, J., Annunziatellis, A., Bekkby, T., Bruschi, A., Doncheva, V., Drakopoulou, V., Duncan, G., Inghilesi, R., Kyriakidou, C., Lalli, F., Lillis, H., Mo, G., Muresan, M., Salomidi, M., Sakellariou, D., Simboura, M., Teaca, A., Tezcan, D., Todorova, V., Tunesi, L., 2017. EUSeaMap. A European broad-scale seabed habitat map. https://doi.org/10.13155/49975

11 Annex 4 - Comparison of four softwares for the union of polygonal layers

Mickaël Vasquez – Ifremer

Mickael.Vasquez@ifremer.fr

Roland Pesch - Bioconsult

roland.pesch@jade-hs.de

11.1 Introduction

This study aimed at comparing the performance of four softwares, namely ArcGIS™, GRASS, QGIS and R for the union of three polygon layers. "Union" in this context means that an intersection of all the layers is performed, and the output layer comprises both the polygons that result from the intersection and the remaining, non-overlapping polygons (figure 11.1).The table of the output layer contains all the fields of the input tables.

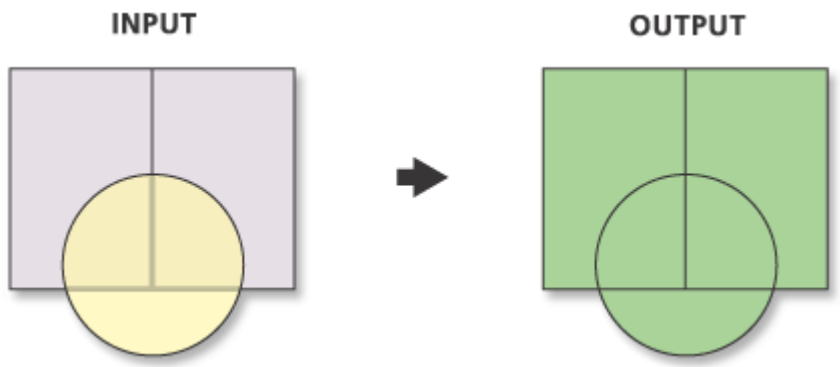

Figure 11.1: Illustration of the union of two layers (from ArcGIS™ 10.2 help). The union of two –polygon features (pink layer) and one polygon feature (yellow) results in a polygon with five features (green).

11.2 Material and methods

11.2.1 Material

Three test datasets were produced. The first one comprised a small number of polygons and aimed to allow for the assessment of the various tools with a simple, easy-to-check example. The two other datasets contained more polygons in order to assess the performance time of the tools.

For each dataset, three layers, referred to hereafter as 'layer 1', 'layer 2' and 'layer 3', were created as input for the union. In the layers each polygon was assigned a class which was described via a code. In the example illustrated in Figure 2, layers 1 and 2 have three classes, and layer 3 has five classes.

The European Marine Observation and Data Network (EMODnet) is financed by the European Union under Regulation (EU) No 508/2014 of the European Parliament and of the Council of 15 May 2014 on the European Maritime and Fisheries Fund.

11.2.1.1 Test dataset 1

The three layers that composed the test dataset 1 are illustrated in Figure 11.2 and their characteristics are summarised in Table 11.1. It should be noted that layers 1 and 2 have the same spatial coverage, while layer 3 has less polygons alongshore.

Table 11.1: Number of polygons and classes in dataset 1 layers

Layer	Number of classes	Number of polygons
1	3	56
2	3	46
3	5	30

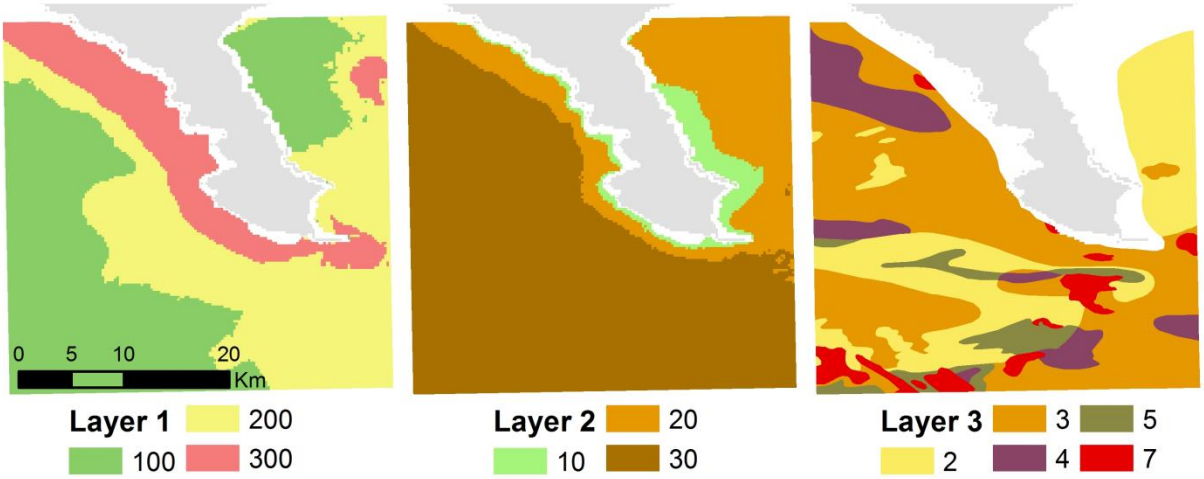

Figure 11.2: The 3 layers that composed the dataset 1 (as a background layer, in grey, is the land)

11.2.1.2 Test dataset 2

The three layers that composed the test dataset 2 are illustrated in Figure 11.3 and their characteristics are summarised in Table 11.2.

Table 11.2: Number of polygons and classes in dataset 2 layers

Layer	Number of classes	Number of polygons
1	4	2288
2	6	21294
3	8	14965

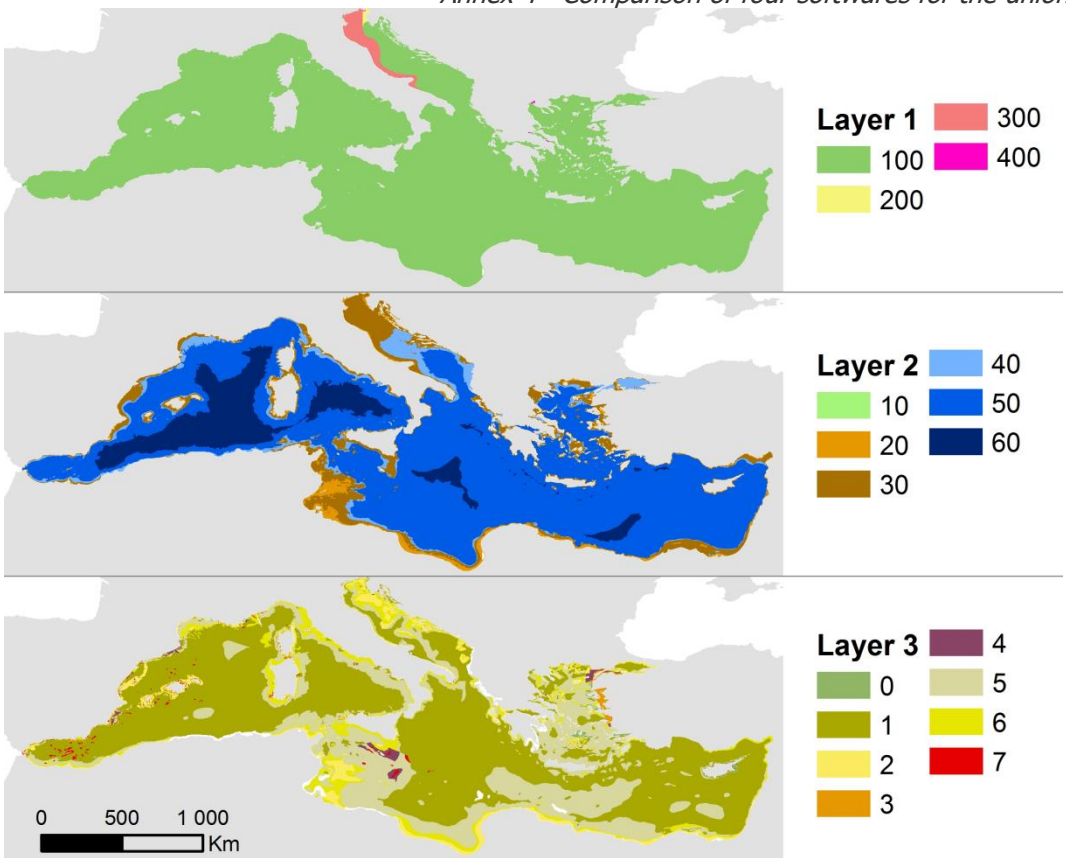

Figure 11.3: the 3 layers that composed the dataset 2

11.2.1.3 Test dataset 3

The three layers that composed the test dataset 3 are illustrated in figure 11.4 and their characteristics are summarised in Table 11.3.

Table 11.3: Number of polygons and classes in dataset 3 layers

Layer	Number of classes	Number of polygons
1	3	30899
2	14	64726
3	8	27353

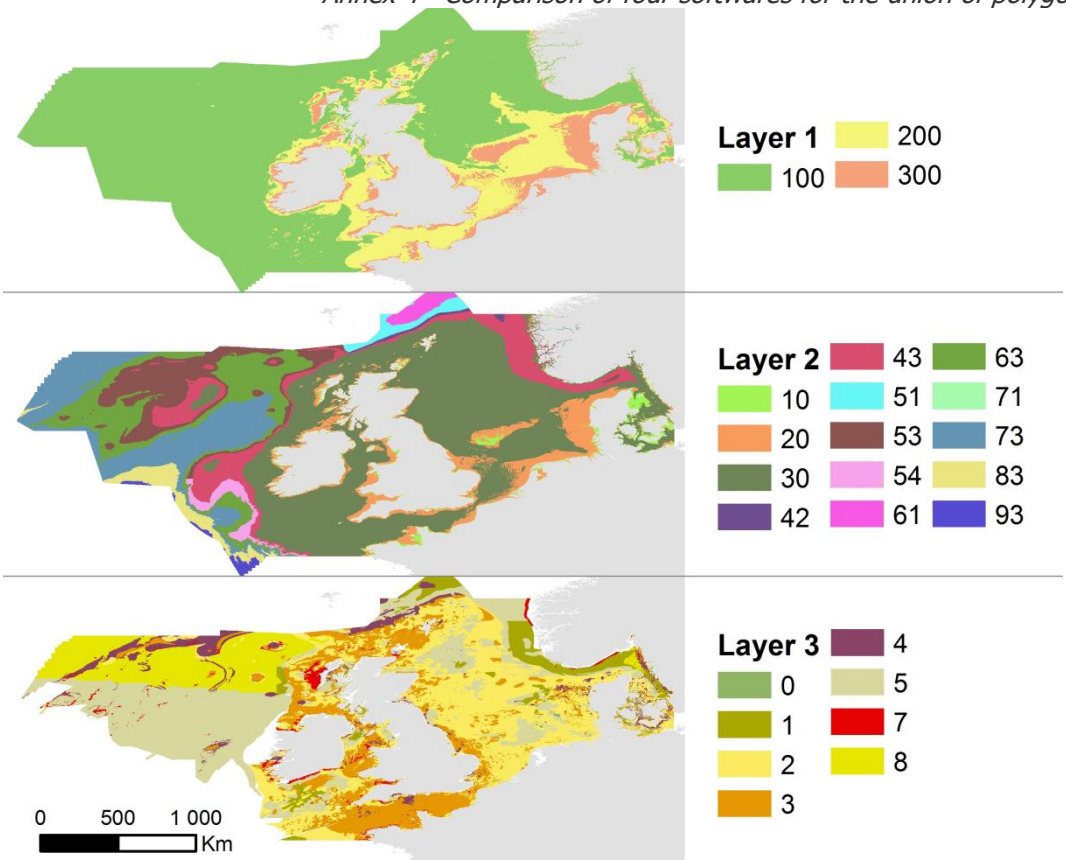

Figure 11.4: the 3 layers that composed the dataset 3

11.2.2 Method

11.2.2.1 Running the tools

The tests were performed on a unique computer, comprising a 3.4GHz quad-core Xeon e3-1245 v3 CPU and 16GB of DDR3 memory, and a st1000dm003-1er162 scsi hard disk. All the input datasets were copied onto the hard drive of the computer. The tools were requested to produce the outputs onto the hard drive.

A summary of the tools/functions that were tested, as well as the software characteristics, are provided in Table 11.4. We tested two R functions provided by 2 different packages. GRASS function was launched from QGIS.

Table 11.4: Tools/functions tested and software characteristics

Software	Version	Tool/function	Toolset/Package
ArcGIS	10.2	Union	Analysis Tools > Overlay
QGIS	2.18.10 64 bits	Union	QGIS geoalgorithms > Vector overlay tool
R	3.1.3 64 bit	gUnion	rgeos
R	3.1.3 64 bit	union	raster
GRASS	7.2.1	v.overlay ('OR' operator)	Launched from QGIS

Python scripts were written to run the QGIS and the GRASS functions, and a R script was written to run the two R functions.

11.2.2.2 Assessing the outputs

The outputs provided by ArcGIS, QGIS, R and GRASS were assessed in three steps.

1) **Was the output complete with regards to the number of fields?** It was checked that the output attribute table had 3 fields named 'code1', 'code2' and 'code3', corresponding to the field 'code1' of layer 1, 'code2' of layer 2, and 'code3' of layer 3 respectively. This step was performed on dataset 1 only. This was based on the assumption that if it was successful or unsuccessful with this dataset, then the same would apply to the other datasets.

2) **Was the output geometry correct?** This step aimed to check that the intersection between multiple polygons generated clean outputs, i.e. a) without minor issues such as null geometries and b) without overlap between polygons. (a) was checked via the ArcGIS™ 10.2 'Check Geometry' tool (in *Data management Tools > Features* toolset). (b) was checked using ArcGIS™ 10.2 Geodatabase topology facilities.

3) **Was the output thematic information exact?** A set of randomly-placed validation points were used to check if the information described in the output layer matched that of the input layers, i.e. pivot tables were produced to check how well the code that was in the output field 'code1' matched the code that was in the field 'code1' of the input layer 1; the code that was in the output field 'code2' matched the code that was in the field 'code2' of the input layer 2; and the code that was in the output field 'code3' matched the code that was in the field 'code3' of the input layer 3. An R script was written to perform this assessment. As an example, the point dataset used for the validation of the outputs produced with the dataset 2 is illustrated in figure 11.5.

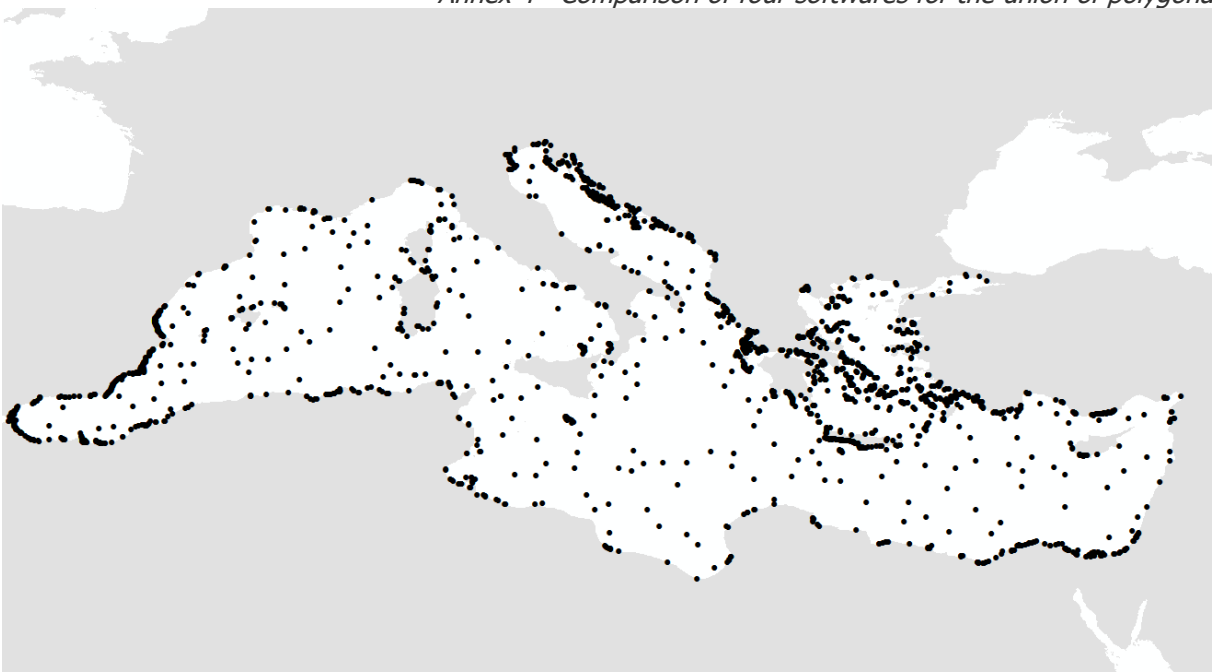

Figure 11.5: Random point data that was used for the dataset 2 in order to assess thematic information exactness of the output resulting from the union of the three layers

11.3 Results

11.3.1 The gUnion R function is too selective regarding topology validity

Working with the dataset 1, the gUnion R function raised an exception error while running the union between layer2 and layer 3.

```
TopologyException: Input geom 0 is invalid: Ring Self-intersection at or near po
int at -4.8479665000000001 54.695857820000001
```

At the location mentioned in the message, there was a tiny isolated polygon in one of the input layers surrounded by much larger polygons. (Figure 11.6, polygon A). It is not obvious that this would be considered as a topological error. Even if it is one, it does not appear to be sufficiently severe to raise an exception error.

The rgeos gUnion function was therefore removed from the test procedure.

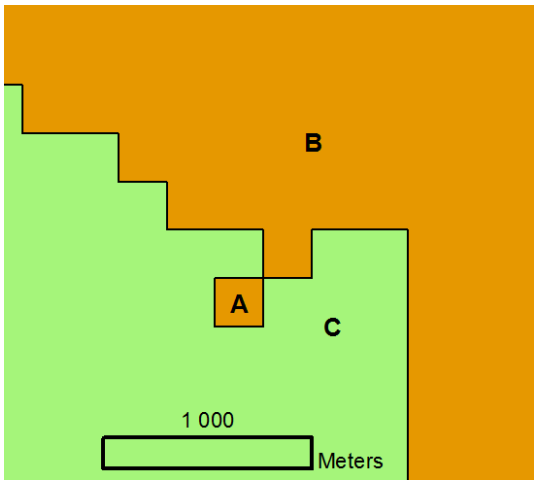

Figure 11.6: Example of topology that led to an exception error with the R gUnion function.

11.3.2 Test with dataset 1

11.3.2.1 Quick look at the outputs

Quick views of the outputs are displayed in Figure 11.7. QGIS, ArcGIS and GRASS outputs looked quite similar, while the output produced by the Union function of the R raster package had massive holes (see blank areas in the right map of Figure 11.7).

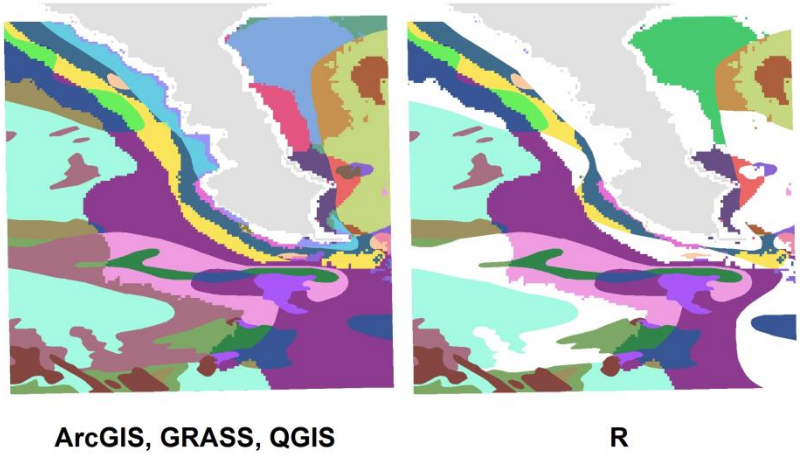

Figure 11.7: Quick views of outputs generated with ArcGIS, QGIS, GRASS and R. Only one quick view is shown for the former three because they looked quite similar, while the R output showed clear massive holes (blank areas).

11.3.2.2 Time performance

Time performances are summarized in table 11.5. QGIS and R were fast, ArcGIS was the most efficient, and GRASS was the least fast.

Table 11.5: Time performances for each tool with dataset 1

Software	Tool/function	Time duration
ArcGIS	Union	Less than 1s
QGIS	Union	2s
R	union	2s
GRASS	v.overlay	7s

11.3.2.3 Was the output complete with regards to the number of fields?

All three tools generated a table with the expected three fields 'code1', 'code2' and 'code3'.

11.3.2.4 Was the geometry correct?

None of the three tools generated overlap errors. But as a result of the 'Check Geometry' tool on the QGIS output, 265 records were detected as either null geometry or self-intersection.

Table 11.6: Output number of polygons, minor issues with geometry and overlaps for each tool.

Software	Tool/function	Output number of polygons	Polygons with minor issues	Overlaps
ArcGIS	Union	183	0	0
QGIS	Union	456	265	0
R	union	149	0	0
GRASS	v.overlay	265	0	0

11.3.2.5 Was the output thematic information exact?

222 random points were used to validate the output values, i.e. to check that the values in the output table fields 'code1', 'code 2' and 'code 3' matched those in the field 'code1' of the layer 1, the field 'code2' of the layer 2, and the field 'code3' of the layer 3. The results showed 100% agreement between the input and the output in ArcGIS, GRASS and QGIS. There was less agreement in the results from R due to the presence of holes in the output (see section 11.3.2.1), the 150 points located in these holes were assigned a <NA> value.

11.3.2.6 Conclusions

ArcGIS, GRASS and QGIS were successful in this first test on a simple dataset, although some minor (and easy to remove) geometry issues were identified in the QGIS output.

Due to the incomplete nature of the output, the union function of the R raster package was deemed inappropriate, and the function was not tested with dataset 2 and 3.

11.3.3 Test with dataset 2

11.3.3.1 Time performance

ArcGIS was quite fast (35 seconds), while QGIS was quite slow (44 hours). GRASS performance time was reasonable (17 minutes).

Table 11.7: Time performances for each tool with dataset 1

Software	Tool/function	Time duration
ArcGIS	Union	35 seconds
QGIS	Union	158,444 seconds (44 hours)
GRASS	v.overlay	1030 seconds

11.3.3.2 Was the geometry correct?

In the ArcGIS output one polygon had self-intersection, and a few overlaps were detected. GRASS also performed well with an output having 39 self-intersections and 53 overlaps. QGIS produced a layer with a large amount of empty geometries (64,923!) and more overlaps than ArcGIS and GRASS.

Table 11.8: Output number of polygons, minor issues with geometry and overlaps for each tool

Software	Tool/function	Output number of polygons	Polygons with minor issues	Overlaps
ArcGIS	Union	128,971	1	70
QGIS	Union	124,563	64,923	194
GRASS	v.overlay	128,892	39	53

11.3.3.3 Was the output thematic information exact?

2,516 random points were used to check that the output values in the field 'code1', 'code 2' and 'code 3' matched those of in the field 'code1' of the layer 1, the field 'code2' of the layer 2, and the field 'code3' of the layer 3. The ArcGIS, GRASS and QGIS output values had full agreement with the input values.

11.3.4 Test with dataset 3

11.3.4.1 Time performance

ArcGIS completed the job in around one minute. GRASS did so in 50 minutes. After 48 hours, QGIS had not completed the first of the two runs. The job was therefore cancelled because it was deemed pointless to let it reach the end.

Table 11.9: Time performances for each tool with dataset 1

Software	Tool/function	Time duration
ArcGIS	Union	65 seconds
QGIS	Union	Cancelled after 48h (not half of the job completed)
GRASS	v.overlay	3000 seconds (50 minutes)

11.3.4.2 Was the geometry clean?

No geometry issue was observed with ArcGIS and GRASS.

Table 11.10: Output number of polygons, minor issues with geometry and overlaps for each tool

Software	Tool/function	Output number of polygons	Polygons with minor issues	Overlaps
ArcGIS	Union	150,908	0	0
QGIS	Union	-	-	-
GRASS	v.overlay	213,385	0	0

11.3.4.3 Was the output thematic information exact?

3,877 points were used to compare the output values of the field 'code1', 'code 2' and 'code 3' and the input ones. For all these points, ArcGIS, GRASS and QGIS output values had full agreement with the input values.

11.4 Conclusions

ArcGIS is the only software that enables the union of more than two layer in one run. This was not critical for the present study because there were only 3 input data layers, but this might be a problem for applications that would have a long list of input data layers.

R options were rapidly removed from the test because they were not successful with the simplest input dataset. The gUnion function provided by the rgeos package was too selective regarding the input topology, thus could not even be run. The union function provided by the R package produced an output with massive irrelevant holes.

QGIS Union function produced outputs that were acceptable. However, some overlaps between polygons were identified, and an impressive number of empty geometries were produced (64,000 with dataset 1). This should be improved.

ArcGIS Union function produced outputs with very few geometric shortcomings with dataset 2, and the outputs produced with datasets 1 and 3 were fully geometrically correct.

GRASS outputs were all excellent regarding geometry. Geometry errors identified for the three datasets ranged from none to few. GRASS is definitely a trustworthy option for polygon data overlaying.

The thematic validity of the outputs was excellent with QGIS, GRASS and ArcGIS. In all three datasets, all the validation points proved that the output values matched the input ones. The three softwares can therefore be used with confidence for that particular aspect.

The main difference between ArcGIS, QGIS and GRASS softwares was observed in the time performance. ArcGIS was surprisingly fast (less than one minutes for datasets 2 and 3), while QGIS was surprisingly slow (44 hours with dataset 2, job cancelled after 48 hours and not even half of the job done) which, considering the high resource capacity of the computer that was used, was far too low and deemed eliminatory. GRASS was substantially slower than ArcGIS but the performance was still acceptable.

In conclusion, ArcGIS and GRASS are currently the best options for the union of layers with a large number of polygons. ArcGIS is substantially better than GRASS when it comes to time performance, whereas GRASS is slightly better than ArcGIS regarding geometry results.

12 Annex 5 - Comparative EUSeaMap 2016 and 2019

12.1 Biological zones

Table 12.1: biological zone total spatial coverage across MSFD regions (or subregions) in km² and in percentage coverage of the region (or subregion)

id	name	spZoneType	area (km2)	area EUSeaMap2016 (km2)	area EUSeaMap2016 (%)	area EUSeaMap2019 (km2)	area EUSeaMap2019 (%)
ABI	Bay of Biscay and the Iberian Coast	MSFDsubregion	803349	787043	97	800127	99
ACS	Celtic Seas	MSFDsubregion	974385	969097	99	968037	99
ACSo	Celtic Seas - overlapping submissions to UNCLOS from UK and Kingdom of Denmark	MSFDsubregion_part	148994	149048	100	148943	99
AMA	Macaronesia	MSFDsubregion	3967476	3354404	84	3485373	87
ANS	Greater North Sea, incl. the Kattegat and the English Channel	MSFDsubregion	654178	641926	98	651403	99
BAL	Baltic	MSFDregion	392214	389018	99	383610	97
BAR	Barents Sea	nonMSFDsea	1948047	359077	18	1126292	57
BLK	Black Sea	MSFDregion	473894	431287	91	432754	91

id	name	spZoneType	area (km2)	area EUSeaMap2016 (km2)	area EUSeaMap2016 (%)	area EUSeaMap2019 (km2)	area EUSeaMap2019 (%)
ICE	Iceland Sea	nonMSFDsea	755844	753350	99	753033	99
MAD	Adriatic Sea	MSFDsubregion	139783	134657	96	139664	99
MAL	Aegean-Levantine Sea	MSFDsubregion	757833	747273	98	757477	99
MIC	Ionian Sea and the Central Mediterranean Sea	MSFDsubregion	773032	762620	98	772943	99
MWE	Western Mediterranean Sea	MSFDsubregion	846002	843094	99	844672	99
NOR	Norwegian Sea	nonMSFDsea	887043	497733	56	562718	63
WHI	White Sea	nonMSFDsea	89442	0	0	72767	81

Table 12.2: EUSeaMap 2016 - Biological zone spatial coverage in km² across MSFD regions (or subregions). MSFD regions' or subregions' full names are in table 12.1

biozone	ABI	ACS	ACSo	AMA	ANS	BAL	BAR	BLK	ICE	MAD	MAL	MIC	MWE	NOR	WHI
Infralittoral	6636	12168	0	3727	24198	61510	3428	15974	7999	6668	21339	42509	13287	4695	0
Shallow circalittoral	40234	55362	0	515	116199	249155	5930	54937	21559	93479	91109	99826	113957	3590	0
Deep circalittoral	90423	381983	329	3752	435156	78353	42935	44874	80356	0	0	0	152	33528	0
Bathyal	111180	338890	93287	371816	66373	0	302248	216675	563010	34510	615356	590103	442197	277771	0
Abyssal	538570	180694	55432	2974594	0	0	4536	98827	80426	0	19469	30182	273501	178149	0

Table 12.3: EUSeaMap 2019 - Biological zone spatial coverage in km² across MSFD regions (or subregions). MSFD regions' or subregions' full names are in table 12.1

biozone	ABI	ACS	ACSo	AMA	ANS	BAL	BAR	BLK	ICE	MAD	MAL	MIC	MWE	NOR	WHI
Infralittoral	6257	10196	0	777	25360	66530	13194	16634	5838	10368	31242	49188	15018	4286	7622
Shallow circalittoral	41363	54378	0	534	114733	238681	78205	50964	23268	96995	95954	112115	107289	3335	47255
Deep circalittoral	89714	378930	331	4073	436978	78399	309665	47158	80371	0	0	0	0	33924	13329
Bathyal	115046	347730	94265	407513	74332	0	720505	217712	569578	32301	611396	581648	448859	315741	4561
Abyssal	547747	176803	54347	3072476	0	0	4723	100286	73978	0	18885	29992	273506	205432	0

12.2 Seabed substrate

Table 12.4: seabed substrate total spatial coverage across MSFD regions (or subregions) in km² and in percentage coverage of the region (or subregion)

id	name	spZoneType	area (km2)	area EUSeaMap2016 (km2)	area EUSeaMap2016 (%)	area EUSeaMap2019 (km2)	area EUSeaMap2019 (%)
ABI	Bay of Biscay and the Iberian Coast	MSFDsubregion	803349	275582	34	272680	33
ACS	Celtic Seas	MSFDsubregion	974385	780265	80	766164	78
ACSo	Celtic Seas - overlapping submissions to UNCLOS from UK and Kingdom of Denmark	MSFDsubregion_part	148994	148951	99	148874	99
AMA	Macaronesia	MSFDsubregion	3967476	1683891	42	1659787	41
ANS	Greater North Sea, incl. the Kattegat and the English Channel	MSFDsubregion	654178	631329	96	638671	97
BAL	Baltic	MSFDregion	392214	386027	98	383424	97
BAR	Barents Sea	nonMSFDsea	1948047	312509	16	895405	45
BLK	Black Sea	MSFDregion	473894	431108	90	431552	91
ICE	Iceland Sea	nonMSFDsea	755844	752406	99	752142	99
MAD	Adriatic Sea	MSFDsubregion	139783	134316	96	136897	97
MAL	Aegean-Levantine Sea	MSFDsubregion	757833	739721	97	748228	98
MIC	Ionian Sea and the Central Mediterranean Sea	MSFDsubregion	773032	762326	98	764248	98

id	name	spZoneType	area (km2)	area EUSeaMap2016 (km2)	area EUSeaMap2016 (%)	area EUSeaMap2019 (km2)	area EUSeaMap2019 (%)
MWE	Western Mediterranean Sea	MSFDsubregion	846002	842727	99	843988	99
NOR	Norwegian Sea	nonMSFDsea	887043	128750	14	132341	14
WHI	White Sea	nonMSFDsea	89442	0	0	72589	81

Table 12.5: EUSeaMap 2016 - Seabed substrate spatial coverage in km² across MSFD regions (or subregions). MSFD regions' or subregions' full names are in table 12.4

substrate	ABI	ACS	ACSo	AMA	ANS	BAL	BAR	BLK	ICE	MAD	MAL	MIC	MWE	NOR	WHI
Rock or other hard substrata	19275	37177	4117	29437	11715	12713	11605	407	14687	713	263	3001	7516	14305	0
Coarse substrate	14443	179912	4080	2151	100382	20312	40439	12313	78550	0	0	0	82	17831	0
Mixed sediment	12139	38754	19348	23814	15046	152871	7308	31043	33254	0	0	0	25	249	0
Coarse and mixed sediment	0	0	0	0	0	0	0	1423	0	538	9084	9356	8747	0	0
Sand	100833	170487	4595	16951	345039	52627	12920	9736	79583	19204	23255	40934	46160	7660	0
Fine mud	28765	35355	0	1586921	51664	36116	18751	300764	19810	57760	397864	408850	512791	26100	0
Posidonia meadows	0	0	0	0	0	0	0	0	0	253	436	5844	5376	0	0
Dead mattes of Posidonia	0	0	0	0	0	0	0	0	0	10	0	15	30	0	0

Table 12.6: EUSeaMap 2019 – Seabed substrate spatial coverage in km² across MSFD regions (or subregions). MSFD regions' or subregions' full names are in table 12.4

substrate	ABI	ACS	ACSo	AMA	ANS	BAL	BAR	BLK	ICE	MAD	MAL	MIC	MWE	NOR	WHI
Rock or other hard substrata	18463	19362	2062	27477	11317	11926	15181	476	14619	629	266	3071	7537	15180	0
Coarse substrate	22601	179906	4165	1478	99617	20688	84123	11862	78523	0	0	0	0	15015	3223
Mixed sediment	7503	38861	20420	23713	14183	149269	28941	42163	33249	39	0	0	0	1351	3
Coarse and mixed sediment	0	0	0	0	0	0	0	227	0	1585	4477	9307	8175	0	0
Sand	99559	163606	28946	13575	327097	53313	60992	6922	79498	18211	24292	41825	47523	6923	33939
Fine mud	28018	38329	0	1573058	52709	40004	33356	310085	19796	58698	380031	408896	517043	26315	2
Posidonia meadows	0	0	0	0	0	0	0	0	0	242	442	5795	4716	0	0
Dead mattes of Posidonia	0	0	0	0	0	0	0	0	0	10	0	18	487	0	0

12.3 MSFD benthic broad habitat types

Table 12.7: MSFD habitat total spatial coverage across MSFD regions (or subregions) in km² and in percentage coverage of the region (or subregion)

id	name	spZoneType	area (km2)	area EUSeaMap2016 (km2)	area EUSeaMap2016 (%)	area EUSeaMap2019 (km2)	area EUSeaMap2019 (%)
ABI	Bay of Biscay and the Iberian Coast	MSFDsubregion	803349	786833	97	799627	99
ACS	Celtic Seas	MSFDsubregion	974385	938324	96	925432	94
ACSo	Celtic Seas - overlapping submissions to UNCLOS from UK and Kingdom of Denmark	MSFDsubregion_part	148994	149045	100	148940	99
AMA	Macaronesia	MSFDsubregion	3967476	3351719	84	3482432	87
ANS	Greater North Sea, incl. the Kattegat and the English Channel	MSFDsubregion	654178	633532	96	641476	98
BAL	Baltic	MSFDregion	392214	386022	98	383418	97
BAR	Barents Sea	nonMSFDsea	1948047	342220	17	1026285	52
BLK	Black Sea	MSFDregion	473894	431106	90	432566	91
ICE	Iceland Sea	nonMSFDsea	755844	752936	99	752668	99
MAD	Adriatic Sea	MSFDsubregion	139783	134651	96	136896	97
MAL	Aegean-Levantine Sea	MSFDsubregion	757833	739717	97	717348	94
MIC	Ionian Sea and the Central Mediterranean Sea	MSFDsubregion	773032	762616	98	763820	98

id	name	spZoneType	area (km2)	area EUSeaMap2016 (km2)	area EUSeaMap2016 (%)	area EUSeaMap2019 (km2)	area EUSeaMap2019 (%)
MWE	Western Mediterranean Sea	MSFDsubregion	846002	843087	99	843981	99
NOR	Norwegian Sea	nonMSFDsea	887043	480354	54	545886	61
WHI	White Sea	nonMSFDsea	89442	0	0	72586	81

Table 12.8: EUSeaMap 2016 – MSFD habitats' spatial coverage in km² across MSFD regions (or subregions). MSFD regions' or subregions' full names are in table 12.7

MSFD_habitat	ABI	ACS	ACSo	AMA	ANS	BAL	BAR	BLK	ICE	MAD	MAL	MIC	MWE	NOR	WHI
Infralittoral rock and biogenic reef	1926	3906	0	1417	1368	4359	309	184	2575	424	625	6022	6161	576	0
Infralittoral coarse sediment	625	1433	0	401	3441	5115	34	5531	1023	147	1442	8	958	2	0
Infralittoral mixed sediment	328	372	0	96	1738	22950	0	3960	181	71	412	41	5	0	0
Infralittoral sand	2721	2725	0	946	13690	14558	7	4638	3111	5072	12868	32939	5452	2	0
Infralittoral mud	870	673	0	11	2120	12094	89	1583	885	951	4729	3497	709	42	0
Circalittoral rock and biogenic reef	6977	14745	0	160	2514	8354	1309	222	2320	549	66	886	1971	1297	0
Circalittoral coarse sediment	6444	20022	0	33	29702	14834	919	6877	6108	129	3086	13	4692	72	0
Circalittoral mixed sediment	5611	1079	0	38	5425	109274	0	11835	472	171	983	3098	49	0	0
Circalittoral sand	13760	12048	0	111	72212	36829	173	5734	10969	28579	28565	52111	30718	17	0
Circalittoral mud	7406	4188	0	1	5086	79578	474	20902	1535	0	0	0	0	173	0
Offshore circalittoral rock and biogenic reef	7456	15699	94	773	5348	0	6023	0	3004	3	0	65	1232	7304	0
Offshore circalittoral coarse sediment	6529	142411	0	195	67235	362	12182	921	19772	3	722	6	705	5719	0
Offshore circalittoral mixed sediment	5521	7876	0	262	7877	20645	805	13923	1387	14	619	852	85	0	0
Offshore circalittoral sand	36864	131116	7	853	258644	1238	5851	5409	36859	7640	4848	7914	20625	3557	0
Offshore circalittoral mud	34048	60449	228	14	90760	55832	7263	27627	19302	0	0	0	22	5674	0
Upper bathyal rock and biogenic reef	2123	1875	2085	6904	2484	0	3285	0	6104	0	0	0	179	5126	0
Upper bathyal sediment	38673	155993	68073	49401	61679	0	257363	0	271312	0	0	0	315	98159	0
Lower bathyal rock and biogenic reef	663	884	749	6600	0	0	645	0	555	0	0	0	0	0	0
Lower bathyal sediment	11277	107849	22366	227130	0	0	11235	0	284708	0	0	0	0	288	0
Abyssal	538570	180694	55432	2974594	0	0	4536	98827	80426	0	19469	30182	273501	178149	0
Indistinct	58441	72287	11	81779	2209	0	29718	222933	328	90898	661283	624982	495708	174197	0

Table 12.9: EUSeaMap 2019 – MSFD habitats' spatial coverage in km² across MSFD regions (or subregions). MSFD regions' or subregions' full names are in table 12.7

MSFD_habitat	ABI	ACS	ACSo	AMA	ANS	BAL	BAR	BLK	ICE	MAD	MAL	MIC	MWE	NOR	WHI
Infralittoral rock and biogenic reef	1974	1949	0	158	1445	4616	343	241	2110	470	660	6028	6172	665	0
Infralittoral coarse sediment	503	1227	0	22	3041	7655	497	5455	759	273	997	11	924	2	247
Infralittoral mixed sediment	374	185	0	27	1660	21295	18	4237	158	628	297	11	10	0	3
Infralittoral sand	2515	1937	0	129	14153	26284	582	4296	2003	4971	14721	36198	6606	2	4294
Infralittoral mud	716	402	0	0	2582	2163	215	2223	655	3174	8743	3817	653	38	2939
Circalittoral rock and biogenic reef	6970	9252	0	153	2646	7127	1835	235	2672	408	42	895	2033	1264	0
Circalittoral coarse sediment	8668	20310	0	36	27936	12302	19991	6105	6325	106	1545	13	4068	33	2171
Circalittoral mixed sediment	2991	961	0	60	5097	108250	960	13618	490	596	729	3053	109	0	0
Circalittoral sand	16399	11155	0	99	69426	33198	14817	1295	11942	25468	25753	50239	31896	16	29639
Circalittoral mud	6295	4815	0	1	6640	23424	7597	23988	1660	4785	20255	18664	8182	155	15405
Offshore circalittoral rock and biogenic reef	7226	6799	83	512	4691	182	8479	0	3029	3	0	702	679	7517	0
Offshore circalittoral coarse sediment	12435	141091	0	166	68639	729	28522	345	19761	0	250	7	585	6015	741
Offshore circalittoral mixed sediment	3468	9352	0	350	7423	19723	17598	22913	1378	20	203	2030	88	0	0
Offshore circalittoral sand	34382	126969	2	228	243390	2756	42709	2348	36871	7382	5843	9516	17685	3330	4
Offshore circalittoral mud	31919	64497	245	6	108377	21152	156895	22598	19301	14161	12668	21470	19690	5678	12582
Upper bathyal rock and biogenic reef	1704	817	927	6347	2533	0	3792	0	6101	0	0	0	0	5731	0
Upper bathyal sediment	37915	154280	66519	42841	68988	0	574274	0	266449	0	0	0	0	100614	4561
Lower bathyal rock and biogenic reef	496	482	380	7093	0	0	694	0	597	0	0	0	0	1	0
Lower bathyal sediment	12075	116817	26426	242915	0	0	11282	0	296103	0	0	0	0	302	0
Abyssal	547747	176803	54347	3072476	0	0	4723	100286	73978	0	18885	29975	273506	205432	0
Indistinct	62855	75332	11	108813	2809	92562	130462	222383	326	74451	605757	581191	471095	209091	0